2017

Manifestations of Symmetry in Polynomial Link Invariants

Kyle Istvan
Louisiana State University and Agricultural and Mechanical College

MANIFESTATIONS OF SYMMETRY IN POLYNOMIAL LINK INVARIANTS

A Dissertation

Submitted to the Graduate Faculty of the
Louisiana State University and
Agricultural and Mechanical College
in partial fulfillment of the
requirements for the degree of
Doctor of Philosophy

in

The Department of Mathematics

by
Kyle Devin Istvan
B.S., University of Georgia, 2010
M.S., Louisiana State University, 2011
May 2017

Acknowledgments

I would like to express my gratitude to Dr. Oliver Dasbach for his unrelenting patience and support, and his encouragement as I investigated knot theory from every which way. Dr. Mustafa Hajij served as a friend, mentor, and collaborator, and I am forever in his debt for his encyclopedic knowledge of the literature related to this dissertation. My collaborator Dr. Qazaqzeh introduced me to the topic of periodic links and allowed me to join his research project, and I am grateful for his patience as he brought me up to speed so that we could work together despite the distance between our respective universities. I am also thankful to all of the topology faculty at Louisiana State University, in particular Dr. Pat Gilmer and Dr. Neal Stoltzfus, who were always available for unscheduled consultations. Everyone in the mathematics department at Louisiana State University helped provide an excellent academic environment, though it is impractical to list them all here. My friends Max, Paul, Neal, Kate, Jesse, and Susan deserve mention for providing moral support over these many years and reminding me that sometimes the distraction of a good home-cooked meal is all it takes to clear one's head. Last but not least, thank you to my mother and father for everything they've done over the years to help get me here.

Table of Contents

List of Figures

Abstract

The use and detection of symmetry is ubiquitous throughout modern mathematics. In the realm of low-dimensional topology, symmetry plays an increasingly significant role due to the fact that many of the modern invariants being developed are computationally expensive to calculate. If information is known about the symmetries of a link, this can be incorporated to greatly reduce the computation time. This manuscript will consider graphical techniques that are amenable to such methods.

First, we discuss an obstruction to links being periodic, developed jointly with Dr. Khaled Qazaqzeh at Kuwait University, using a model developed in [4]. We will discuss useful corollaries of this new method that arise when applying the criterion to multi-component links, and give a survey of its effectiveness when applied to low-crossing links.

The second part will investigate a structure that arose in the model of [4], namely *singular* links. We first define an invariant of singular links. We then develop a method based on the work of Turaev in [24, 26, 8] and expanded in [19] that allows for the creation of operator invariants from R-matrices. Finally, we show that the invariant defined previously is the natural extension of the Kauffman Bracket, when viewed through this framework.

In the final section we investigate torus links, and relate the values of the Tail of the Colored Jones Polynomials of links within this family. This chapter involves well-known q-series, first studied by Ramanujan, and an unexpected combinatorial series related to planar integer partitions. This work was inspired by two seemingly unrelated questions of Robert Osburn and Oliver Dasbach. The first asked how the tails of two different links might be related, once one recognized that their

Tait graphs have some shared structure. The latter asked if there might be a deletion/contraction type formulation for the Tail of the Colored Jones Polynomial, as it relates to the Tait graph of a link. This work is being done jointly with Mustafa Hajij at the University of South Florida.

Chapter 1
Introduction

A tame ***knot*** is a smooth topological circle sitting inside $\mathbb{R}^3$, or its compactification S^3. These objects are considered up to an equivalence relation called ambient isotopy: that is, an isotopy of the ambient space ($\mathbb{R}^3$ or S^3) that takes one knot to another. Heuristically, one can think of a knot as a tangled piece of (infinitely flexible) string that has had its ends glued together, preventing it from being untied. Any attempt to untie the string by stretching, shrinking, loosening, tugging, twisting, etc. is an example of an ambient isotopy. So, it is not so much the string that we are concerned with, as the *way that it is embedded in space.* A ***link*** is a disjoint union of knots, considered up to the same equivalence. In this paper, the terms knot and link will be used for both an equivalence class and a representative; the use should be clear from context.

Traditionally, knots and links are represented by projecting the image of the embedded circles onto a plane. We require that this projection is injective except at a finite number of double points, each of which is a transverse intersection of two arcs of the knot. The relative height information at a crossing is given by leaving a gap in the arc that is closer to the plane of projection. See the examples below in Figure 1.1.

A basic question in knot theory is to determine when two given links are the same. In order to achieve this, topologists have defined a number of invariants, or quantities that can be associated to a link that do not vary by choosing a different representative of the same equivalence class. A simple example of this is the crossing number: this is the minimum number of double points (crossings) appearing in *any*

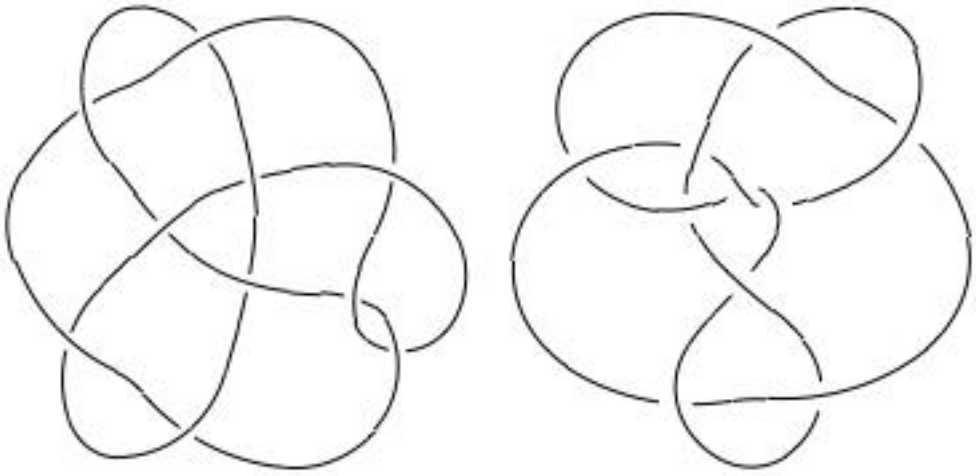

FIGURE 1.1: Knots 10_{101} and 10_{105}

diagram of the link. It should be immediately clear that this is not a very useful definition, however, because there are infinitely many diagrams representing any knot. In fact, we can always increase the number of crossings in a diagram by adding a kink to it at some point, an operation known as a Reidemeister I move. The interested reader should consult [14] for a more thorough background in basic knot theory. One ubiquitous result, however, is the Reidemeister Theorem. This states that two link diagrams represent links that are ambient isotopic if and only if they are are related by a finite sequence of Reidemeister moves, described below in Figure 1.2, as well as planar isotopies.

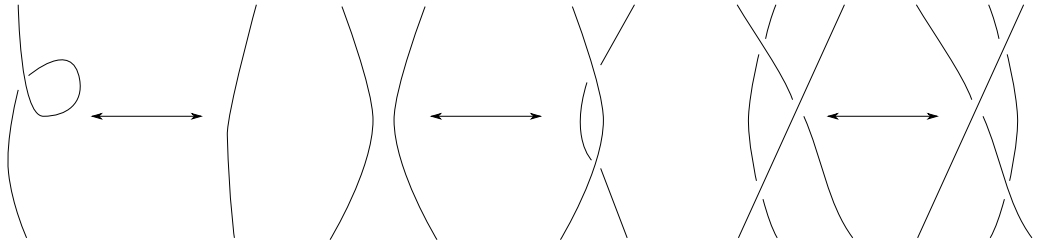

FIGURE 1.2: Reidemeister Moves I, II, and III.

This theorem allows us to check if a quantity that can be calculated from a diagram is an invariant of links. One need only determine that the quantity remains unchanged if a diagram is altered by any of the three Reidemeister moves.

The form that an invariant takes can vary wildly. Some, such as the crossing number, are simply natural numbers. Others, such as the ones that we will be concerned with in this manuscript, are polynomials, Laurent polynomials, or formal power series. There are still others that are groups, entire homology theories, or special elements inside a homology theory. These will sometimes appear throughout the discussion herein, but the details are outside the scope of this work. An excellent summary of some of these invariants can be found in [14].

There are three particular knot invariants that will be used in this document. The first is called the Jones polynomial. This was first defined in 1984 by Vaughn Jones, and sparked the development of the field of quantum topology. The other two invariants can be thought of as two different generalizations of the Jones polynomial. The Kauffman Polynomial will be used to create an obstruction for the periodicity of a link. We will then proceed to look at the colored Jones polynomial, and the Tail of the Colored Jones polynomial, for links with known symmetry. Each of these invariants uses the Kauffman Bracket as a fundamental building block, so that will be our starting point.

Chapter 2
Background

2.1 The Kauffman Bracket

Although originally defined algebraically, there is a diagrammatic description of the Jones polynomial that will be more useful for our purposes. The Kauffman bracket is a function that takes an oriented link diagram and returns a Laurent polynomial in $\mathbb{Z}[A, A^{-1}]$. It can be understood to operate on a link diagram by making local changes, according to the following rules:

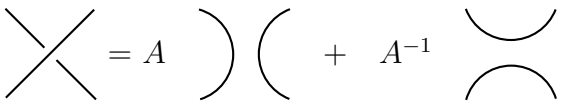

(2.1)

$$L \cup \bigcirc = (-A^2 - A^{-2})L \tag{2.2}$$

where the second relation consists of a link diagram L that is disjoint from a crossingless unknot. The bracket polynomial is also often normalized so that the value of the unknot is 1.

The first of these diagrammatic relations should be interpreted as making a local change on the diagram, where everything away from a small neighborhood of a crossing remains fixed. Note that the second rule should be interpreted as follows: if there is a crossingless, unlinked component of the diagram, it can be removed at the expense of introducing the coefficient $(-A^2 - A^{-2})$.

It can be shown by direct calculation that the Kauffman Bracket is invariant under type II and III Reidemeister moves on diagrams. However, a Reidemeister I move (the addition or removal of a kink) introduces a factor of $-A^{\pm 3}$. To get

a true link invariant, we compensate for this by multiplying by a correction term using the writhe of a diagram. Writhe can be easily read off of a diagram by adding the number of positive crossings and subtracting the number of negative crossings. Using these rules, the Jones polynomial $V_L(A)$ is defined below.

$$V_L(A) = (-A^3)^{-w(L)}\langle L \rangle. \tag{2.3}$$

Without this adjustment, the Kauffman Bracket is still an invariant of *regular isotopy*, or an invariant of framed knots. These will be described in more detail in the following section. At this point, it is worth pointing out that there are several versions of the polynomials that we will be using herein, but they are all the same up to a change of variables. When defined this way, the Jones polynomial is actually a Laurent polynomial in $A^{\pm 2}$. For the purpose of maintaining consistency across the chapters of this text, we will not make the obvious conversion to $v = A^{1/2}$.

2.2 Framed Links

Let us return for a moment to the discussion of the non-invariance of the Kauffman bracket under the Reidemeister I move. It turns out that the appropriate domain for the Kauffman bracket is the set of *framed links*. These are links that come equipped with a nonvanishing normal vector field. The magnitude of these vectors is unimportant; only their direction is relevant to the idea of a framed link. Effectively, one can think of a framed knot as a ribbon that has been tangled and glued together in such a way that it is an orientable surface. Mathematically, this is an embedded annulus, as compared to an embedded circle for an unframed knot. One of the boundary components of this annulus is identified with the knot, and the other will be called the transverse pushoff of the knot. This notion will be important

in both the discussion of the Colored Jones polynomial and the definition of the Kauffman polynomial, so we will go into some detail here.

There is an analogous version of ambient isotopy for framed links in which the framing (normal vector field) is also allowed to vary. It should be intuitively clear that the framing somehow has to wind around the knot some integer number of times, since the "ribbon" ends must glue flat together. To make this precise, note that the first homology of the complement of a knot in S^3 is $\mathbb{Z}$. There are two useful methods to show this fact. One can consider the Wirtinger presentation (see [11]) of the fundamental group of the knot complement, and note that all of the relations are commutators. In the abelianization, each relation thus becomes an equivalence of two of the generators. With a little bit of work, it can then be shown that all generators are equivalent. A faster, but perhaps less enlightening proof, is given by recognizing that the image of a knot in S^3 is a compact, locally contractible subspace. A quick application of Alexander Duality yields the desired result.

Using this fact, the notion of "winding" around the aforementioned knot corresponds to calculating the value of the transverse pushoff as an element of the first homology of the knot complement, yielding an integer. It should be noted that this requires a choice of generator for $\mathbb{Z}$. If the knot has an orientation, we traditionally choose this to agree with the right hand rule; looking along the knot, a positive meridian (generator of the first homology) will wind clockwise around the knot. With this understanding, a framed knot can be represented as an oriented knot together with an integer, with the latter defining the framing.

It is often convenient to represent framed links via diagrams in which they have the blackboard framing. This means that the normal vector field is always parallel to the plane of projection. One might note that the Reidemeister II and III moves

can be performed on such a diagram without changing the framing. Reidemeister I moves, on the other hand, cannot be applied to a diagram without forcing the framing to leave the plane of projection. For blackboard framed link diagrams, the Reidemeister I move is replaced by a relation in which two opposite kinks are added or removed simultaneously, thus preserving the blackboard framing.

One should now observe that the Kauffman Bracket polynomial defined above is invariant under this augmented Reidemeister I, II, and III moves. As such, we can think of it as an invariant of framed links, sometimes called an invariant of *regular isotopy.* In order to get an invariant of traditional knots (the Jones Polynomial), the writhe correction term was required to account for the twisting and untwisting that occurs as a knot diagram is decomposed via the Kauffman relations.

2.3 Periodic Links

A link in S^3 is called ***n-periodic*** if there is an order n homeomorphism of the 3-sphere that fixes the link setwise, but fixes no point on the link. It is known that the fixed point set of such a map must be itself a copy of S^1, and furthermore that this circle is unknotted. This latter fact is due to the proof of the Smith Conjecture, a problem whose resolution took several decades. Using this fact, a periodic knot can be considered to be a diagram in the plane with a finite-order rotational symmetry about a point in the plane that is disjoint from the diagram. As an example, the two knots represented by diagrams in Figure 2.1 both represent periodic knots: the first is 3-periodic, as the diagram is invariant under rotation by 120 degrees about a point in the center face. The latter diagram is similarly 2-periodic.

It is useful to point out that this diagrammatic description of n-periodicity does not mean that a link can be represented by the closure of a braid of the form β^n, where the center of the rotational symmetry is understood to represent the braid

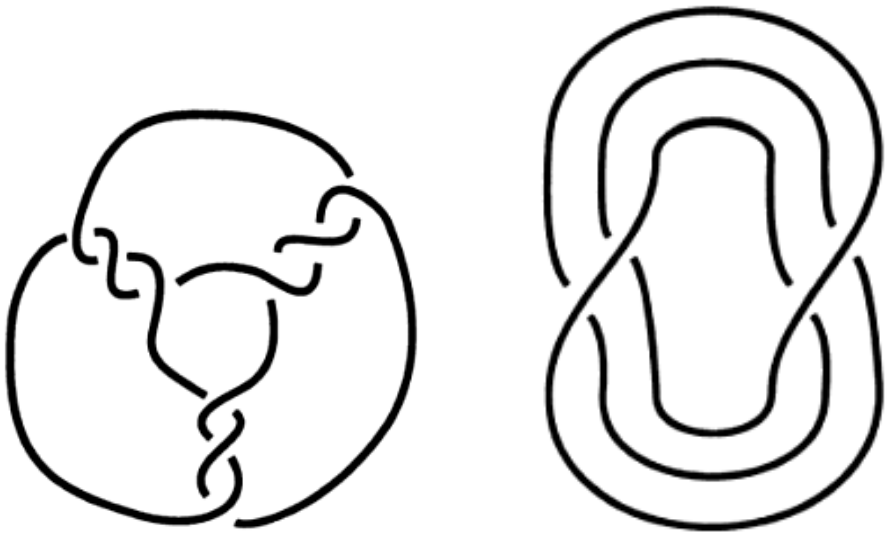

(a) 3-periodic knot (b) 2-periodic knot

FIGURE 2.1: Periodic Knot Diagrams

axis. The key observation is that while there is necessarily a diagram that is a product of n copies of a tangle, there is nothing requiring that the strands always flow around the braid axis in the same direction. A periodic diagram may have strands that locally wind both clockwise and counterclockwise with respect to the fixed point of symmetry.

Given any composite positive integer $n = ab$, the natural inclusion of the cyclic symmetry groups $\mathbb{Z}/_{a\mathbb{Z}}$ and $\mathbb{Z}/_{b\mathbb{Z}}$ into $\mathbb{Z}/_{n\mathbb{Z}}$ immediately yields that an n-periodic link will also be a- and b-periodic. As such, this manuscript will follow the common convention of restricting the study of periodic links to positive prime periodicities.

2.4 Kauffman Polynomial

The Kauffman Polynomial is a 2 variable polynomial, of which the ordinary Jones polynomial is a special case. To see Kauffman's original description, we refer the reader to [13].

This text will use a second definition that utilizes a diagrammatic state sum description first given in [4]. The advantage of this version is that its states can

be obtained similarly to those of the Kauffman Bracket polynomial. The difference is the addition of a third term to the first Kauffman relation 2.1, as shown in Equation 2.4. Here, A and B are taken to be distinct commuting variables.

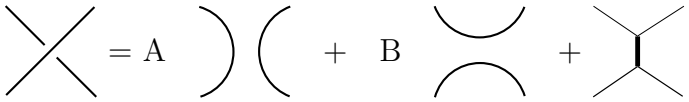

(2.4)

After resolving all crossings of a diagram with c crossings, we are left with a formal linear combination of 3^c diagrams, each consisting of planar trivalent graphs and simple closed curves. These graphs come equipped with an associated perfect matching on the vertices, depicted by the thickened edges in the diagrams of Equation 2.4.

To each state, we associate a polynomial in 3 variables A, B, and a that we will call the *Graph Polynomial* and denote by $P(\Gamma)$, where Γ refers to a single state diagram. This is again defined diagrammatically using the five properties listed in Equations 2.5 - 2.9. It is no trivial task to show that these rules yield a well-defined polynomial, and we refer the reader to the original source [4] for such details. It should be noted at this point that the details of the definition of the Graph Polynomial are not important for the purposes of this paper. The reader need only pay attention to the coefficients, and observe that the Graph Polynomial is invariant under planar isotopies, including rotations in the plane.

$$P(\Gamma \cup \bigcirc) = \quad \alpha P(\Gamma) \tag{2.5}$$

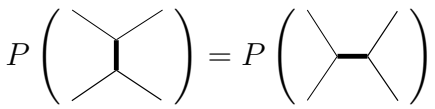

(2.6)

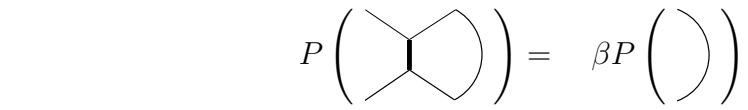

(2.7)

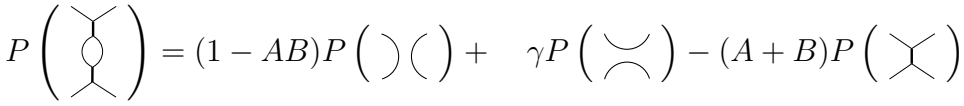

(2.8)

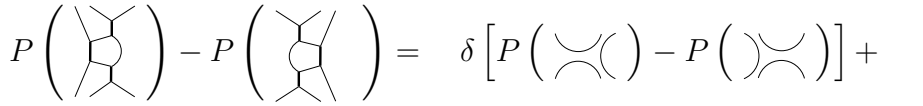

(2.9)

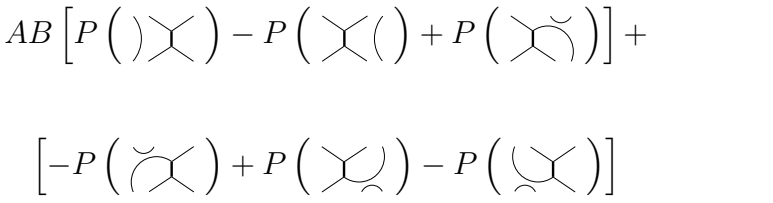

where

$$\alpha = \frac{a - a^{-1}}{A - B} + 1 \tag{2.10}$$

$$\beta = \frac{Aa^{-1} - Ba}{A - B} - A - B \tag{2.11}$$

$$\gamma = \frac{B^2 a - A^2 a^{-1}}{A - B} + AB \tag{2.12}$$

$$\delta = \frac{B^3 a - A^3 a^{-1}}{A - B} \tag{2.13}$$

Here, it should be pointed out that the definitions of these coefficients prohibit the specialization $A = B$, thus necessitating the previous stipulation that A and B be distinct variables. The factor of $A - B$ in these denominators will play an important role in choosing a specialization of this polynomial in Section 3.1.

To a diagram D, we can now associate a *Total Graph Polynomial* as follows:

$$\Lambda_D(a, A - B) = \sum_{\Gamma} A^{(\#A)} B^{(\#B)} P(\Gamma) \tag{2.14}$$

where $\#A$ and $\#B$ represent the number of A- or B-smoothings used to generate the state graph Γ. Combining all of this, we can finally state the result of [4].

Definition 2.1. *The Kauffman polynomial of an oriented link L with diagram D is given by*

$$F_L(a, z) = (-1)^{|L|+1+w(D)} \Lambda_D(-ia, iz) \tag{2.15}$$

where $|L|$ represents the number of components of the link, $w(D)$ represents the writhe of the link diagram, and i is the usual complex fourth root of unity.

2.5 Tail of the Colored Jones Polynomial

The Colored Jones polynomial is a sequence of Laurent polynomial invariants generalizing the Jones polynomial. In essense, the n^{th} Colored Jones polynomial of a framed link is computed by considering specific linear combinations of Kauffman Brackets of *cables* of the link diagram, in which each strand of a link is replaced by n parallel copies. Here, it is important to note that "parallel" indicates that the copies are all transverse pushoffs of the original link; that is, they exist in the direction of the framing of the link. We will assume that all link diagrams are equipped with the blackboard framing.

It should be immediately clear that the n-cabled versions of the Reidemeister II and III moves are still invariant under the Kauffman Bracket. The Reidemeister I move, however, again creates a problem, in that an R-I move on the uncabled diagram corresponds to a full twist of the n parallel strands in the cabled diagram, introducing n^2 new crossings and throwing the framing out of the plane of projection. Whereas in the case of the Jones polynomial we were able to fix this

by simply accounting for the writhe, the solution in the case of the Colored Jones polynomials is considerably more complex.

We will not go into details here, but a detailed description can be found in [10]. We are concerned with a quantity called the Tail that can sometimes be associated to this sequence of polynomials. For a given link, the Tail reflects the stabilization of coefficients in the sequence of Colored Jones polynomials. The Tail was shown to exist for adequate links in [6].

Fix an adequate link. To define the Tail, let us first define a sequence of polynomials, denoted the *shifted Colored Jones polynomials* $\{sCJP\}_n$, by multiplying each element in the sequence of Colored Jones polynomials by an appropriate power of A so that each resulting polynomial has a positive constant as its lowest-degree nonzero term. The Tail is the formal power series with the property that its $4n^{th}$ coefficient agrees with that of sCJP_m for every integer $m \geq n$.

The final chapter of this document will be concerned with identities that arise when looking at the tails of $(2, k)$-torus knots and links, and will make use of the natural 2- and k-periodic symmetry of these objects.

Chapter 3

The Kauffman Polynomial and Periodic Links

3.1 An Obstruction to Periodicity

The following section details work completed in collaboration with Dr. Khaled Qazaqzeh of Kuwait University.

We present a method to detect the obstruction of p-periodicity for links, using the Kauffman polynomial. This uses the aforementioned fact that periodicity of a link must manifest in the existence of a diagram with rotational symmetry. Combining that fact with Caprau and Tipton's state sum description of the Kauffman polynomial, we are able to show that symmetry in a diagram will force the Kauffman polynomial to contain a symmetric factor, and use this to create the following congruency between the Kauffman polynomials of a link and its mirror image.

Theorem 3.1. *Let p be prime. If L is a p-periodic link with mirror image L', then*

$$F_L(iq, iq - iq^{-1}) \equiv F_{L'}(iq, iq - iq^{-1}) \quad mod(p, q^{2p} - 1) \tag{3.1}$$

It should be noted at this point that this fact was already shown by Przyticki in a different form. See Theorem 1.4 in [20]. However, the following proof uses new techniques, and yields a result that is easily computed using existing software from the KnotTheory package for Mathematica. Sample code and a summary of calculations are included in Appendix A.

The above evaluation of the Kauffman Polynomial corresponds to the specializations $a = B = q$ and $A = q^{-1}$. The reason for this choice will become clear in the course of proving the theorem. Before we proceed with the proof, let us examine some immediate consequences and limitations of this theorem.

This theorem has one immediate limitation, in that it does not allow us to garner any information for amphichiral links. It can also be seen that we will gain no information for the case where $p = 2$, corresponding to evaluating the Kauffman polynomial at fourth roots of unity. It is worth noting that in practice, the congruency has held true for every example computed when $p = 3$, suggesting that evaluating the specialized Kauffman Polynomial at sixth roots of unity may detect some property of links that is invariant under taking the mirror image. Thus, this theorem is not useful for the two smallest primes. The difficulty of determining which knots are 3-periodic is ubiquitous in the literature; it is only relatively recently that some techniques involving Heegaard-Floer Homology were able to complete (with one exception) 3-periodicity data in the knot tables up to 12 crossings, and there are still unknown entries for 13 and higher crossing knots. See [12] for more information.

Before giving an example, let us first show the following.

Proposition 3.2. *Consider the specialization of Kauffman Polynomial as in Theorem 3.1 as a Laurent polynomial in $q^{\pm 1}$. For a link L and its mirror image L', we have that $F_L(q) = F_{L'}(q^{-1})$.*

Proof. The proof makes use of two facts shown in [14] as Proposition 16.1, parts (i) and (iii). The first states that the Kauffman polynomial remains unchanged if we change the signs of both arguments of the function simultaneously. Part (iii) states that the Kauffman Polynomial of the mirror image can be obtained from that of the original link by inverting the variable a (the first argument of the function).

Applying both of these facts immediately yields the desired equivalence:

$$\begin{aligned} F_L(q) &= F_L(iq, iq - iq^{-1}) \\ &= F_L(-iq, iq^{-1} - iq) \\ &= F_{L'}((-iq)^{-1}, iq^{-1} - iq) \\ &= F_{L'}(iq^{-1}, iq^{-1} - iq) \\ &= F_{L'}(q^{-1}) \end{aligned}$$

□

The following example shows how the theorem can be used to investigate the possible symmetries of the trefoil knot.

Example 3.3 (Trefoil)**.**

$$F_K(a, z) = (-2a^2 - a^4) + (a^3 + a^5)z + (a^2 + a^4)z^2$$

This specializes to

$$F_K(iq, iq - iq^{-1}) = 4q^4 - 2q^6 - 2q^2 + 1$$

Similarly,

$$F_{K'}(iq, iq - iq^{-1}) = 4q^{-4} - 2q^{-6} - 2q^{-2} + 1$$

One can check that these are equivalent modulo the ideal generated by $(p, q^{2p} - 1)$ *only if* $p = 2, 3$*. Hence, we conclude that the trefoil knot can only be 2- or 3-periodic. Recognizing that the trefoil is the (2,3) torus knot, we immediately see that it does in fact have both of these symmetries.*

Example 3.4. *We can use this criterion to show that:*

- *The knot* 10_{101} *in Figure 1.1 is not 7-periodic, confirming the result of Traczyk in [22].*

- *Similarly,* 10_{105} *in Figure 1.1 is not 7-periodic, a result first showed by Murasugi in [18].*

We can use another property of the Kauffman Polynomial to our advantage, which is that it is in fact an invariant of *oriented* links. In the case of links with multiple components, we have the following useful fact:

Proposition 3.5. *If a link fails the criterion for periodicity for any choice of orientation, then none of its oriented versions are p-periodic.*

Proof. To see this, we refer to Proposition 16.4 in [14], which when adapted to the current specialization states the following:

Proposition 3.6. *If the oriented link* L_* *is obtained from the oriented link* L *by reversing the orientation of a single component* K*, then the resulting Kauffman Polynomial is related via*

$$F_{L_*} = q^{4lk(K,L-K)} F_L \tag{3.2}$$

where lk represents the linking number.

Observe that for a p-periodic diagram, the linking number will always be divisible by p. Thus, the two polynomials are related by some power of q^{2p}, which reduces to 1 when we quotient out modulo $(p, q^{2p} - 1)$. □

This proposition turns out to be quite interesting, as shown by the following examples:

Example 3.7. *For $p = 5$, exactly one of the oriented versions of each of the following links is obstructed: L6a3, L7a2, L8a10, L8a13, L8n1. Thus, none of these links can be 5-periodic.*

We see that in the case of links with $|L|$ components, we get up to $2^{|L|}$ possible obstructions to periodicity, and they are not trivially related to one another.

Looking at Definition 2.1 and using the fact that both the number of components and the parity of the writhe are equivalent between a link diagram and its mirror image, we see that it suffices to prove Theorem 3.1 at the level of the Total Graph Polynomial.

Proof. Suppose that L is a p-periodic link, where p is a prime integer. We can then choose a diagram D with c crossings representing L that is symmetric by rotation by an angle of $\frac{2\pi}{p}$ about a point disjoint from the knot. Consider the set of states that are obtained when resolving this diagram according to Relation 2.4.

Lemma 3.8. *Any non-p-periodic state diagram (ie, one that is not invariant under rotations by $\frac{2\pi}{p}$), considered up to rotation in the plane, must appear p times in the set of 3^c states.*

Proof. The cyclic symmetry group $\mathbb{Z}/p\mathbb{Z}$ naturally acts on the set of states in the resolution tree by rotating each state by $\frac{2\pi}{p}$. The orbit of a non-p-periodic diagram must contain more than one distinct state. Because p is a prime number, the Orbit-Stabilizer Theorem allows us to conclude that the size of the orbit must be p. □

Every state in an orbit of the above action will have the same coefficient in the state sum, since they are all obtained from the same number of A- and B-resolutions. Since the Graph Polynomial is independent of planar isotopy (including

rotation in the plane), we can thus group together the states by orbits, noting that the coefficients of non-p-periodic states will be divisible by p. When we reduce the polynomial $mod(p)$, these terms will disappear.

As such, we see that we need only consider the contributions from the p-periodic states. The existence of these states is guaranteed by our hypothesis that our link is p-periodic. To understand the behavior of these states, we begin with the following lemma.

Lemma 3.9. *For a p-periodic state, the exponents $\#A$ and $\#B$ in the associated coefficient in the definition of the Total Graph Polynomial will each be divisible by p.*

Proof. Consider the orbits of the crossings in D under the action of the rotation group, similar to the proof of the previous lemma. These orbits will necessarily have size p, because D was chosen to be a p-periodic diagram. As such, if a crossing is given an A-resolution (resp. B-resolution) in a p-periodic state, every crossing in its orbit must also have been resolved in the same manner. Thus, the total number of A- and B-resolutions must each be a multiple of p. □

We now turn our attention to the specialization given in the statement of the theorem, namely that $a = B = q$ and $A = q^{-1}$. The reasons for this choice can now be elucidated. Firstly, note that the common denominator $A - B$ that appears in the coefficients of the Graph Polynomial will take the nonzero form $q^{-1} - q$, as necessary. In fact, the denominators disappear entirely, so we know that we don't need to worry about interference when we mod out by the quotient ideal. Secondly, consider the effect of applying the previous lemma under this specialization. We can rewrite the definition of the Total Graph Polynomial in the form

$$\Lambda_D(q, q^{-1} - q) \equiv \sum_{\Gamma_p} q^{p(m-n)} P(\Gamma_p) \quad mod(p) \tag{3.3}$$

where $\#A = pn$, $\#B = pm$, and Γ_p is used to indicate that we are only summing over the p-periodic states.

Due to the interchangeability of the pieces in Relation 2.6, we can see immediately the effect of computing this polynomial on the mirror image D' of the diagram, as follows:

$$\Lambda_{D'}(q, q^{-1} - q) \equiv \sum_{\Gamma_p} q^{p(n-m)} P(\Gamma_p) \quad mod(p) \tag{3.4}$$

where the states are indexed in the same order as the corresponding sum for the diagram D.

Combining these, we get that

$$\Lambda_D(q, q^{-1} - q) - \Lambda_{D'}(q, q^{-1} - q) \equiv \sum_{\Gamma_p} (q^{px} - q^{-px}) P(\Gamma_p) \quad mod(p) \tag{3.5}$$

where $x = m - n$.

It remains only to be shown that the coefficients $(q^{px} - q^{-px})$ always vanish when we reduce modulo $(q^{2p} - 1)$. The ideal is generated by the linear factors of the form $(\omega - 1)$ where ω is a $2p^{th}$ root of unity. Since each of these is also a root of the coefficient $(q^{px} - q^{-px})$, we see that the coefficient exists within the ideal, and thus the difference of the Total Graph Polynomials of a p-periodic link and its mirror image vanishes when we reduce modulo $(p, q^{2p} - 1)$.

□

3.2 Transition to Singular Links

Let us briefly return to the defining relations for the Graph Polynomial, specifically Equation 2.6. Combining this with Equation 2.4, we see that it does not in fact matter whether we resolve the crossing into a trivalent graph piece horizontally or vertically. Once could thus express all of the relations defining the Graph Polynomial instead using 4-valent graphs. As we compute the resolution tree for a given link, then, we arrive at intermediate diagrams that can be viewed as representing *singular links*. This alternative interpretation of the computation of the Kauffman Polynomial leads us to naturally wonder if it is somehow an extension of the Jones Polynomial that incorporates information about all of the singular links that can be created from a given diagram. This provides the motivation for the following chapter, in which we investigate a method to extend the Jones Polynomial to singular knots. The methods are not unique to the Jones Polynomial, but other invariants will not be studied in depth within this text.

Chapter 4
An Invariant of Singular Links

Singular knots and links can be regarded as 4-regular graphs with rigid vertices embedded in the 3-sphere, considered up to ambient isotopy. They can be represented by singular link diagrams in the same manner as traditional links, except that singular link diagrams will include true double-points for the vertices of the graph. The specification that these embedded graphs have rigid vertices is best understood by thinking of a singular link diagram as a link diagram in which some of the crossing information has been forgotten; at such a crossing, we wish to maintain the transverse nature of the double point.

This rigidity condition makes singular link diagrams difficult to distinguish. We will prove, for example, that the singular trefoil seen in Figure 4.1 is distinct from its mirror image.

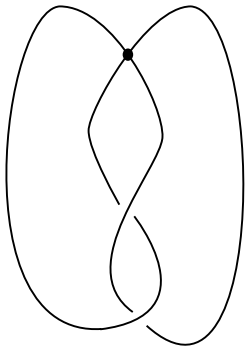

FIGURE 4.1: Singular Trefoil

This portion of the manuscript will consist of three sections. In the first, an invariant of singular links will be defined in a manner similar to the Kauffman Bracket polynomial previously defined for knots, and a proof of its invariance will be given. In the following section, the techniques developed in [24, 26, 8, 19] for

constructing quantum link invariants using tangle operators will be adapted for singular links. In the final section we will show that the invariant defined in the first section is in fact an extension of the Kauffman Bracket polynomial, and thus can be thought of as a singular Kauffman Bracket. At an intermediate step, we also recover a set of representations of the singular braid monoids. It should be noted that there have been other successful, distinct attempts to extend the Jones polynomial to singular links. The interested reader is referred to [7].

Before proceeding, we will need a version of the Reidemeister Theorem for singular links:

Theorem 4.1. *Two singular link diagrams represent isotopic singular links if and only if they are related by a finite sequence of local moves shown in Figure 4.2, as well as planar isotopies.*

The first three of these are the traditional Reidemeister moves, sufficient to determine if a quantity is a knot invariant. The latter three extend the theorem for singular link diagrams. Observe that if we are merely requiring that our invariant be an invariant of *regular* isotopy, as is the case with the Bracket Polynomial, we need not check the move RI, but instead the augmented version in which two opposite kinks are simultaneously introduced or removed.

4.1 Bracket Polynomial for Singular Links

Define the singular bracket function $J_s(D)$ to take singular link diagrams as input, and output a Laurent polynomial in two variables. As before, it satisfies the following relations:

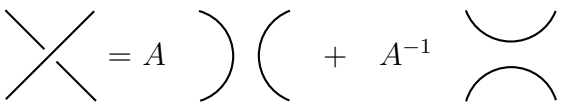

(4.1)

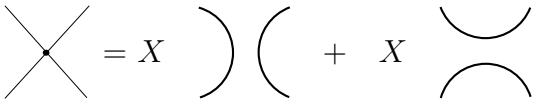

(4.2)

$$L \cup \bigcirc = (-A^2 - A^{-2})L \tag{4.3}$$

This definition is identical to the definition of the Kauffman Bracket, with the addition of Relation 4.2 describing how to resolve singular crossings. Observe that the new variable X need not be invertible; this is a desirable property when dealing with singularities, and in fact is the basis of the work in the following section.

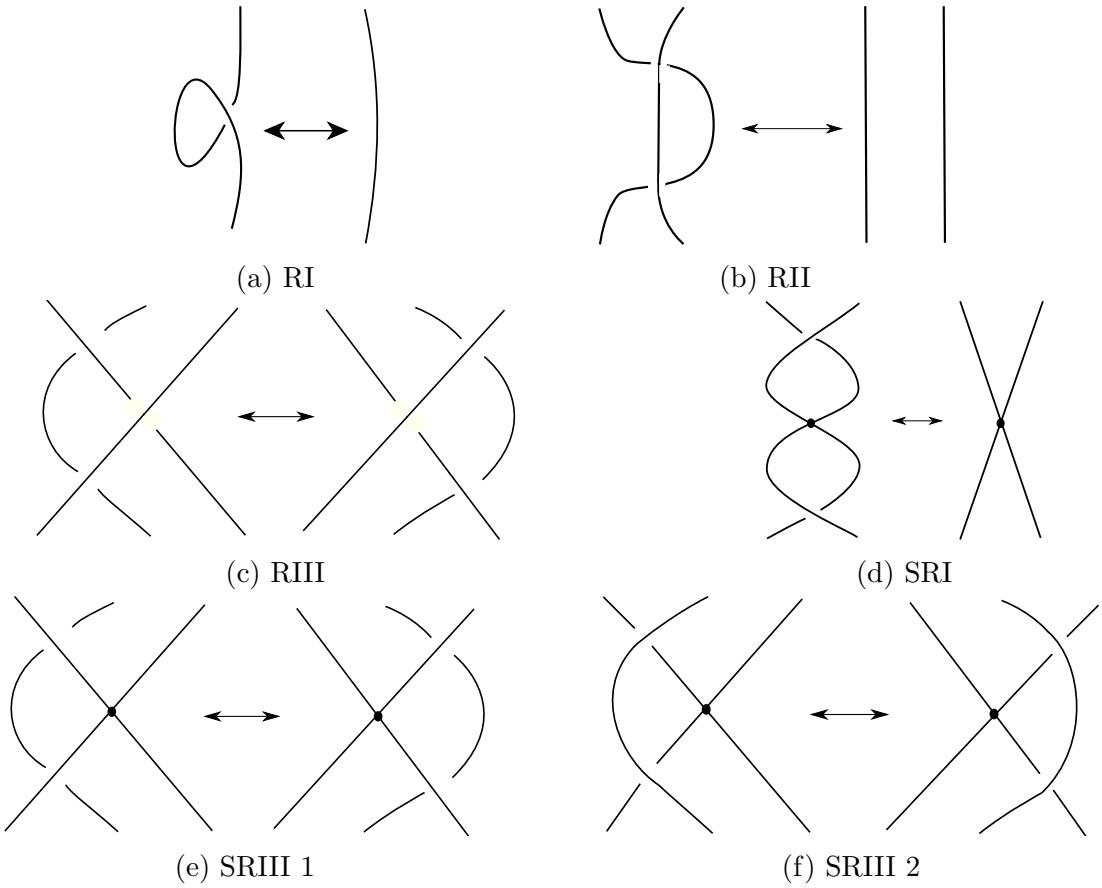

(a) RI (b) RII

(c) RIII (d) SRI

(e) SRIII 1 (f) SRIII 2

FIGURE 4.2: Singular Reidemeister Moves

To those that have spent time working with the Kauffman Bracket, it should be immediately clear that the exponent of X after resolving the crossings will simply

be the number of singularities in the original diagram. The resolution of crossings with the invertible variable A, however, means that while the singular relation is simple, it allows us to distinguish very similar knots.

Example 4.2. *Consider the singular trefoil T shown in Figure 4.1. The Singular Bracket polynomial takes a value of*

$$J_s(T) = \delta(\delta + 1)X(A^2 + 2 + \delta A^{-2})$$

whereas its mirror image yields

$$J_s(T') = \delta(\delta + 1)X(\delta A^2 + 2 + A^{-2})$$

where $\delta = (-A^2 - A^{-2})$.

Thus, we can see that these two singular knots are distinct.

We proceed to show that this definition will truly yield a regular isotopy invariant of singular framed knots.

Proof. The fact that the Singular Bracket Polynomial is invariant under the first two moves and the augmented first move was discussed in the introduction. We will show the invariance for SRI and SRIII-1 only, as the proof for SRIII-2 is similar. Let us consider the evaluation of the left hand diagram of SRI, by first resolving the singular crossing using Relation 4.2:

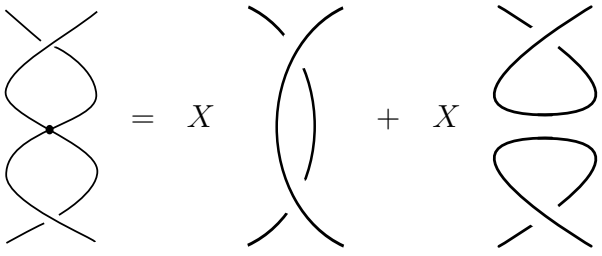

To the first of these diagrams we can apply the move RII, and to the second an augmented RI. We thus get

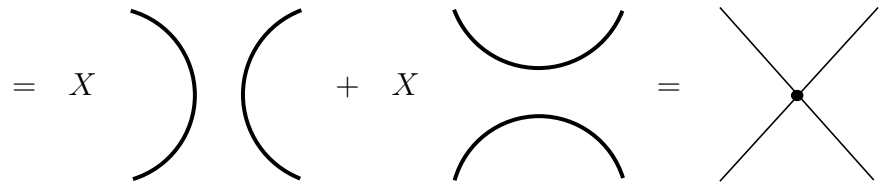

as desired.

The proof for the SRIII-1 move will proceed similarly; we will begin by resolving the singular crossing, and proceed with a sequence of RII moves to achieve the desired result.

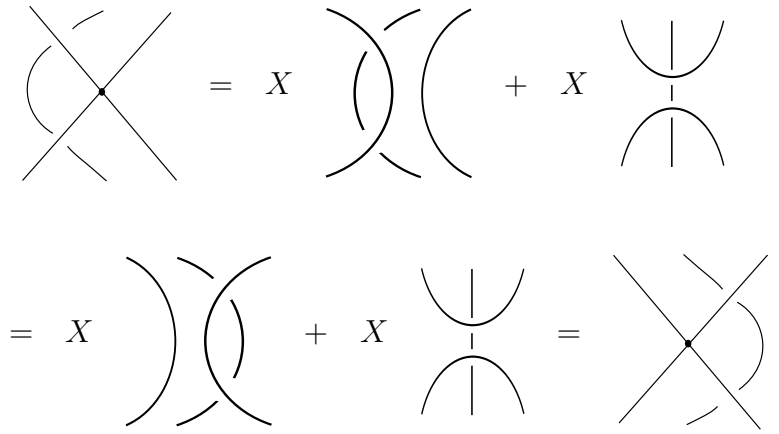

□

This gives a simple diagrammatic method to calculate a singular link invariant. In the following section, we will turn our attention to a more general method of constructing such invariants, and show that the one we have constructed appears as a natural extension of the Kauffman Bracket polynomial.

4.2 A Singular Quantum Tangle Operator Invariant

In this section, we will adapt the methods outlined in [19] to construct singular link invariants using R-matrices. First, it will be useful to have a brief discussion of how link diagrams can be represented by operators acting on some vector space. Throughout this section, we will let $\mathbb{K}$ denote a ground field (usually taken to be

$\mathbb{C}$), and V will denote a vector space. For a given diagram, we will color the arcs by vector spaces to represent the path taken by a vector as it passes through a series of operators. A linear map $R : V \otimes V \to V \otimes V$ may be represented, for example, via the diagram in Figure 4.3d. We similarly have its inverse in Figure 4.3e, a "cap" operator $n : V \otimes V \to \mathbb{K}$ in Figure 4.3a, a "cup" operator $u : \mathbb{K} \to V \otimes V$ in Figure 4.3b, the identity map $\mathbb{I} : V \to V$ in Figure 4.3c, and singular map $R_s : V \otimes V \to V \otimes V$ in Figure 4.3f.

These six maps have corresponding diagrams, which we will call *elementary singular tangles*, and complete a set of simple pieces into which any singular link diagram may be decomposed. These building blocks are combined similarly to the way elements of the braid group can be represented by stacking generator diagrams, each of which takes the form of a single crossing juxtaposed by vertical strands. In this setting, juxtaposition will correspond to tensoring the associated vector spaces, and composition of linear maps will correspond to vertically stacking the associated diagrams. Link diagrams, as such, will be read from bottom to top.

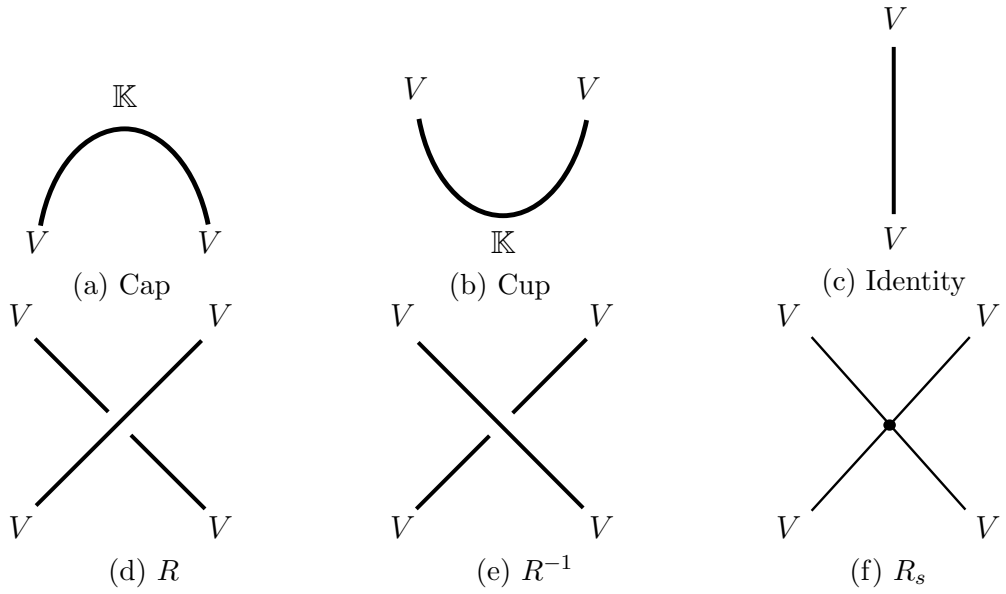

(a) Cap (b) Cup (c) Identity

(d) R (e) R^{-1} (f) R_s

FIGURE 4.3: Elementary Tangles

An excellent example of the operator corresponding to a link diagram can be seen on p. 48 of [19].

We would like to give a process by which we can use a diagram to create an operator in such a way that we can recover some invariant quantity (determinant, trace, etc) that will be independent of our choice of link diagram. For this to be the case, we must check that the maps R, R^{-1}, R_s, u and n satisfy the relations of the Singular Reidemeister Theorem 4.1, shown in Figure 4.2. We must be careful here; while these conditions are necessary, they do not yet form a sufficient set of relations to guarantee an invariant. The key observation is that we are now viewing the cup and cap pieces as operators, and must therefore check that planar isotopies involving these pieces do not change the operator.

A full list of the relations that must be satisfied for classical links was given by Turaev et. al. in [24, 26, 8] and is summarized in Theorem 3.1 of [19]. For singular knots, we need only include singular versions of those relations, to arrive at the following theorem:

Theorem 4.3. *Two singular tangle decompositions represent the same singular tangle if and only if they are related by a finite sequence of the singular Turaev moves listed here:*

1. *The five moves RII, RIII, SRI, SRIII-1 and SRIII-2 illustrated in Figure 4.2.*

2. *The classical Turaev moves illustrated in Figure 3.4 of [19].*

3. *The "Singular Cap Switch" illustrated in Figure 4.4.*

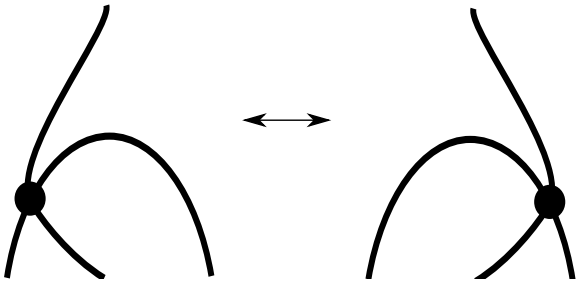

FIGURE 4.4: Singular Cap Switch

There is no need for a corresponding "Singular Cup Switch", as this can be realized using a combination of the other moves.

The moves involving the new singular map R_s are expressed algebraically in Equations 4.4 - 4.7.

$$RR_sR^{-1} = R_s \tag{4.4}$$

$$(R^{-1} \otimes \mathbb{I})(\mathbb{I} \otimes R_s)(R \otimes \mathbb{I}) = (\mathbb{I} \otimes R)(R_s \otimes \mathbb{I})(\mathbb{I} \otimes R^{-1}) \tag{4.5}$$

$$(R \otimes \mathbb{I})(\mathbb{I} \otimes R_s)(R^{-1} \otimes \mathbb{I}) = (\mathbb{I} \otimes R^{-1})(R_s \otimes \mathbb{I})(\mathbb{I} \otimes R) \tag{4.6}$$

$$(\mathbb{I} \otimes n)(R_s \otimes \mathbb{I}) = (cap \otimes \mathbb{I})(\mathbb{I} \otimes R_s) \tag{4.7}$$

We are now able to extend known invariants of classical knots and links to invariants of singular links via the following theorem, analogous to Theorem 3.4 in [19]. The three conditions listed are exactly those required to guarantee a link invariant.

Theorem 4.4. *Let $R : V \otimes V \to V \otimes V$ and $n : V \otimes V \to \mathbb{K}$ be operators satisfying the three conditions*

$$nR = n \tag{4.8}$$

$$(\mathbb{I} \otimes n)(R^{\pm 1} \otimes \mathbb{I}) = (n \otimes \mathbb{I})(\mathbb{I} \otimes R^{\pm 1}) \tag{4.9}$$

$$(R \otimes \mathbb{I})(\mathbb{I} \otimes R)(R \otimes \mathbb{I}) = (\mathbb{I} \otimes R)(R \otimes \mathbb{I})(\mathbb{I} \otimes R) \tag{4.10}$$

If an operator R_s can be found satisfying Relations 4.4 through 4.7, then the associated operator corresponding to a tangle decomposition of a link diagram is an isotopy invariant of the singular link.

We see by construction that such a singular link invariant immediately restricts to an invariant of classical links.

4.3 Singular Bracket Polynomial as a Tangle Operator

The R-matrices and caps associated to several well-known invariants have been discovered, including those for the Alexander polynomial and the Kauffman Bracket polynomial. We will focus on the Kauffman Bracket polynomial, and proceed to show that one choice of an extended singular link invariant guaranteed by Theorem 4.4 is the same as the Singular Bracket polynomial defined in the Section 4.1, up to a specialization of variables.

First, we outline the well-known maps from p. 51 of [19]

$$R = \begin{bmatrix} A & 0 & 0 & 0 \\ 0 & 0 & A^{-1} & 0 \\ 0 & A^{-1} & A - A^{-3} & 0 \\ 0 & 0 & 0 & A \end{bmatrix} \tag{4.11}$$

$$n = \begin{bmatrix} 0 & A & -A^{-1} & 0 \end{bmatrix} \tag{4.12}$$

$$u = \begin{bmatrix} 0 \\ -A \\ A^{-1} \\ 0 \end{bmatrix} \tag{4.13}$$

that yield the Kauffman Bracket. We define a singular operator matrix

$$R_s = \begin{bmatrix} x & 0 & 0 & 0 \\ 0 & f & \frac{x-f}{A^2} & 0 \\ 0 & \frac{x-f}{A^2} & \frac{f+(A^4-1)x}{A^4} & 0 \\ 0 & 0 & 0 & x \end{bmatrix} \tag{4.14}$$

for non-invertible elements x and f.

A straightforward computation will confirm that these pieces satisfy all of the conditions of Theorem 4.4 except for Equation 4.7. Before attempting to resolve this final relation, let us pause and consider the structure that has been forced upon this operator. It turns out that in its current form, we can construct a representation of the singular braid monoid $\mathbb{B}_n$ on n strands.

Definition 4.5. *The singular braid monoid on n strands is the monoid generated by the elements* $\sigma_1, \ldots, \sigma_{n-1}, \sigma_1^{-1}, \ldots, \sigma_{n-1}^{-1}, \tau_1, \ldots, \tau_{n-1}$ *subject to the following relations:*

1. *For all* $1 \leq i < n$,
   (a) $\sigma_i \sigma_i^{-1} = \sigma_i^{-1} \sigma_i = e =$ *identity*
   (b) $\sigma_i \tau_i \sigma_i^{-1} = \tau_i$
2. *For* $|i - j| > 1$,

(a) $\sigma_i\sigma_j = \sigma_j\sigma_i$

(b) $\sigma_i\tau_j = \tau_j\sigma_i$

(c) $\tau_i\tau_j = \tau_j\tau_i$

3. For all $1 \leq i \leq n-2$,

(a) $\sigma_i\sigma_{i+1}\sigma_i = \sigma_{i+1}\sigma_i\sigma_{i+1}$

(b) $\tau_i\sigma_{i+1}\sigma_i = \sigma_{i+1}\sigma_i\tau_{i+1}$

(c) $\tau_{i+1}\sigma_i\tau_{i+1} = \sigma_i\sigma_{i+1}\tau_i$

For a fixed n, define a map $\phi_n : \mathbb{B}_n \to Hom(V^{\otimes n}, V^{\otimes n})$ by giving its action on the generators:

- $\phi_n(\sigma_i) = \mathbb{I}^{\otimes(i-1)} \otimes R \otimes \mathbb{I}^{\otimes(n-i-1)}$
- $\phi_n(\sigma_i^{-1}) = \mathbb{I}^{\otimes(i-1)} \otimes R^{-1} \otimes \mathbb{I}^{\otimes(n-i-1)}$
- $\phi_n(\tau_i) = \mathbb{I}^{\otimes(i-1)} \otimes R_s \otimes \mathbb{I}^{\otimes(n-i-1)}$

This gives a representation of the singular braid monoid. As this object lies somewhat outside of the scope of this text, however, we will simply note this as an interesting corollary and return to the our discussion of singular link invariants.

We wish to determine how the tangle operator defined above compares with the Singular Bracket polynomial defined in the first section of this chapter. It is already known that it satisfies the non-singular relations, so we need only check that the relation involving a singular crossing agrees between the two definitions.

Let us decompose R_s into a linear combination of two other operators:

$$\begin{bmatrix} x & 0 & 0 & 0 \\ 0 & f & \frac{x-f}{A^2} & 0 \\ 0 & \frac{x-f}{A^2} & \frac{f+(A^4-1)x}{A^4} & 0 \\ 0 & 0 & 0 & x \end{bmatrix} = x \begin{bmatrix} 1 & 0 & 0 & 0 \\ 0 & 1 & 0 & 0 \\ 0 & 0 & 1 & 0 \\ 0 & 0 & 0 & 1 \end{bmatrix} + \frac{x-f}{A^2} \begin{bmatrix} 0 & 0 & 0 & 0 \\ 0 & -A^2 & 1 & 0 \\ 0 & 1 & -A^{-2} & 0 \\ 0 & 0 & 0 & 0 \end{bmatrix} \quad (4.15)$$

This equation is perhaps more illuminating if we express the matrices in terms of known quantities:

$$R_s = x(\mathbb{I}_2 \otimes \mathbb{I}_2) + \frac{x-f}{A^2}(n \otimes u) \quad (4.16)$$

Diagrammatically, this equation takes the form

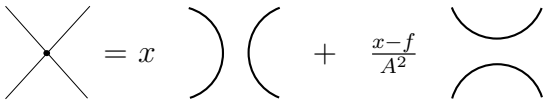

(4.17)

Setting $f = x(1 - A^2)$, we see that this becomes exactly the desired Relation 4.2 in the definition of the Singular Bracket polynomial. The last remaining condition is to see that under this specialization, the operator R_s satisfies the singular cap switch move Equation 4.7, which a straightforward computation will confirm.

Details on these computations are included in Appendix B. The Mathematica code also gives a general computational method for determining the singular extension of any traditional tangle operator, given the corresponding R-matrix, cup, and cap operators.

It should be noted that there is another version of this tangle operator theory for links that uses *oriented* tangles. It may prove worthwhile to attempt to extend this to the world of singular links.

Chapter 5

Relations of Tails of the Colored Jones Polynomial of Torus Links

5.1 Temperley-Lieb Algebra

The Kauffman Bracket relations 2.1 and 2.2 can be used to investigate framed links in a general 3-manifold M. In order to do this, we must clarify the second relation 2.2: Given a link L and an unknot that bounds a disk in M, where the disk is disjoint from L, we can remove the unknotted component at the expense of the coefficient $(-A^2 - A^{-2})$. This condition involving the disk is automatic when dealing with link diagrams in S^3, but in other manifolds it is possible to have diagrams that are unknotted in the plane, yet represent curves that are nontrivial in the fundamental group of M.

The set of links in a manifold, considered up to an equivalence given by the Kauffman Bracket relations, forms an algebraic object known as the Kauffman Bracket Skein Module of the manifold. Let us make this precise:

Definition 5.1. *(J. Przytycki [21] and V. Turaev [25]) Let F be an oriented surface with boundary, and $M = F \times [0,1]$ an oriented 3-manifold. Let R be a commutative ring with identity and a fixed invertible element A. Let $\mathcal{L}_M$ be the set of isotopy classes of framed links in M including the empty link, and note that these can be represented by link diagrams in F by projecting the link onto $F \times 0$. Let $R\mathcal{L}_M$ be the free R-module generated by the set $\mathcal{L}_M$. Let $K(M)$ be the smallest submodule of $R\mathcal{L}_M$ that is generated by all expressions of the form given by Relations 2.1 and 2.2. The Kauffman bracket skein module, $\mathcal{S}(M; R, A) = \mathcal{S}(F; R, A)$, is defined to be the quotient module $\mathcal{S}(M; R, A) = R\mathcal{L}_M / K(M)$.*

In general there is no need to require that M be an extruded surface, but this extra structure yields several useful properties that we will take advantage of in this manuscript.

Observe that if we take the surface $F = D^2$ to be a disc, the associated $\mathcal{S}(D^2; R, A)$ simply equates each framed link diagram with its evaluation using the Kauffman Bracket.

Topologically, we can represent $D^2 = I \times I$ as a product of intervals. Let us consider a set of $2n$ marked points $\{x_1, \ldots, x_{2n}\}$ on the boundary of F, so that the first n points lie on $I \times \{0\}$ and the latter n points lie on $I \times \{1\}$.

Definition 5.2. *The n^{th} Temperley-Lieb Algebra TL_n is the relative Kauffman Bracket Skein Module generated by tangles in D^2 whose endpoints lie on the set of marked points. Addition is defined to be a formal operation on diagrams. Multiplication is given by vertically concatenating diagrams so that the marked points $\{x_1, \ldots x_n\}$ of one diagram coincide with the points $\{x_{n+1} \ldots x_{2n}\}$ of the other.*

Viewed as a vector space, TL_n has a basis consisting of the set of all crossingless matchings of the marked points, because any crossings or link components in a diagram may be removed using the skein relations. See Figure 5.1 as an example of the basis for TL_3.

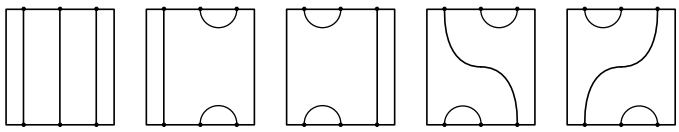

FIGURE 5.1: Basis of TL_3

Viewed as an algebra, TL_n is generated by the much smaller set of $(n-1)$ hooks $\{e_i\}$ shown in Figure 5.2 together with the identity diagram $\mathbb{I}_n$ in which all points are connected via vertical tangles. By multiplying these appropriately, one

can create any crossingless diagram. For instance, the rightmost basis diagram in Figure 5.1 is the product e_1e_2.

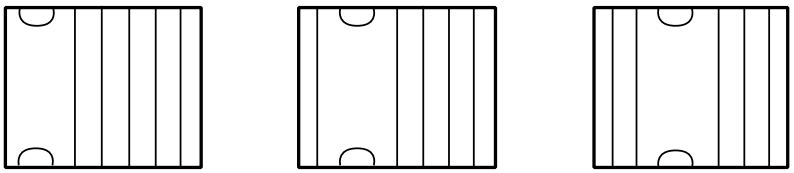

FIGURE 5.2: Hooks e_1, e_2, and e_3 in TL_7.

For any $1 < n < m$ there are very natural inclusions of TL_n into TL_m, given by simply mapping an element T in TL_n to $\mathbb{I}_k \otimes T \otimes \mathbb{I}_{m-n-k}$, where the tensor product represents horizontal concatenation of diagrams. Unless otherwise specified, assume that any inclusions refer specifically to the case where $k = 0$.

For every n, there is a special element f^n inside TL_n called the Jones-Wenzl Idempotent that we represent graphically using a box, as in Equation 5.1. The labelling of strands in the following diagrams indicates a group of parallel strands, equal in number to the label. The Jones-Wenzl Idempotent is defined recursively as follows:

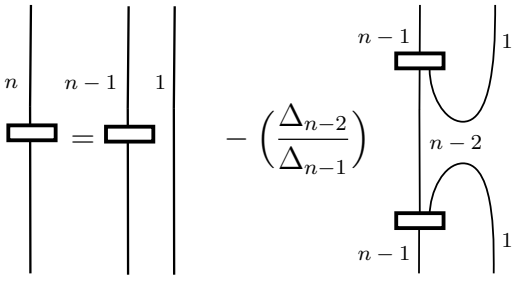

(5.1)

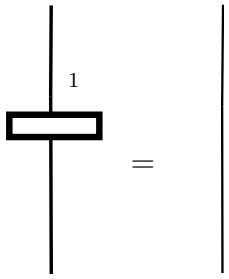

(5.2)

where Δ_n is related to the quantum integer $[n+1]$ via

$$\Delta_n = (-1)^n \frac{A^{2(n+1)} - A^{-2(n+1)}}{A^2 - A^{-2}} = (-1)^n [n+1]. \tag{5.3}$$

We shall let f^0 denote the empty diagram.

The Jones-Wenzl Idempotent satisfies the following properties:

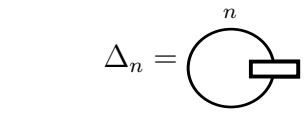

(5.4)

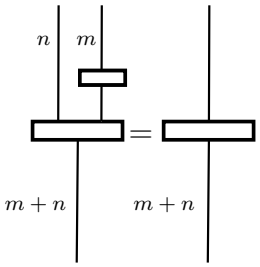

(5.5)

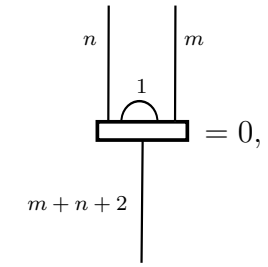

(5.6)

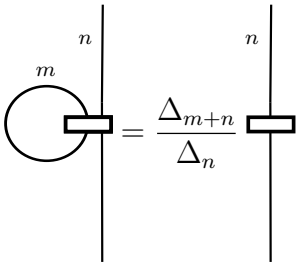

(5.7)

5.2 The Tail of the Colored Jones Polynomial as an Element of TL_n

When discussing the Tail of the Colored Jones polynomial, we traditionally write the polynomials in the variable $q = A^4$, as this is the natural setting for the stabilizing coefficients. For the sake of consistency with the rest of this document, all calculations will continue to use the variable A, but it should be recognized

that we are really only concerned with every 4^{th} coefficient in the polynomials that follow.

Given a blackboard-framed link diagram, we can associate a skein element of $S(D^2, \mathbb{Q}(A^{\pm 1}), A)$ according to the following process. First, resolve all crossings in the manner of the B-smoothing (corresponding to the coefficient A^{-1} in Relation 2.1), and label all strands n. Wherever there was a crossing in the original diagram, insert a copy of f^{2n} that straddles the two smoothed arcs.

In [6], Armond and Dasbach showed that the first n terms in the tail of the Colored Jones polynomial of a link depend only on this specific skein element, easily constructed from a link diagram. In the case of torus knots and links, this element takes a very regular form, which can be seen in the first and third diagrams appearing in the proof of Theorem 5.6. Note that to get the tail of the reduced Colored Jones polynomial, we must divide the value of this skein element by Δ_n.

After the discovery of the Tail of the Colored Jones polynomial, it was quickly noticed that the tails of $(2, k)$-torus knots and links coincided with some well-known q-series [1]. These results are summarized below, beginning with the definition of some common functions.

The q-Pochhammer symbol is given by

$$(a;q)_n = \prod_{k=0}^{n-1}(1 - aq^k) \tag{5.8}$$

The evaluation of the Θ skein element seen in Figure 5.3 is

$$\Theta(i,j,k) = (-1)^{i+j+k}A^{-2(i+j+k)}\frac{(A^4;A^4)_i(A^4;A^4)_j(A^4;A^4)_k(A^4;A^4)_{i+j+k+1}}{(1-A^4)(A^4;A^4)_{i+j}(A^4;A^4)_{i+k}(A^4;A^4)_{j+k}} \tag{5.9}$$

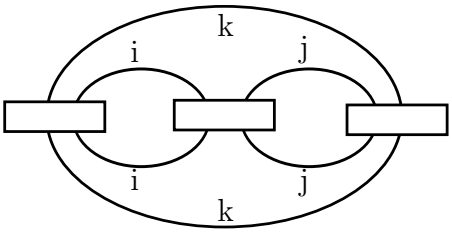

FIGURE 5.3: The Theta Skein Element

This is equivalent to the "trihedron coefficient" $\langle a, b, c \rangle$ defined in [15] via the transformation

$$\langle a, b, c \rangle = \Theta\Big(\frac{a+b-c}{2}, \frac{b+c-a}{2}, \frac{a+c-b}{2}\Big)$$

We will maintain consistency in this chapter and use only the version defined herein.

The Ramanujan Theta function is defined as

$$\begin{aligned} f(a,b) &= \sum_{k=-\infty}^{\infty} a^{\frac{k(k+1)}{2}} b^{\frac{k(k-1)}{2}} \\ &= \sum_{k=0}^{\infty} a^{\frac{k(k+1)}{2}} b^{\frac{k(k-1)}{2}} + \sum_{k=1}^{\infty} a^{\frac{k(k-1)}{2}} b^{\frac{k(k+1)}{2}} \qquad (5.10) \\ &= (-a; ab)_\infty (-b; ab)_\infty (ab; ab)_\infty \end{aligned}$$

It is known in particular that $f(-q^2, -q) = (q; q)_\infty$.

The False Theta function is given by

$$\Psi(a,b) = \sum_{k=0}^{\infty} a^{\frac{k(k+1)}{2}} b^{\frac{k(k-1)}{2}} - \sum_{k=1}^{\infty} a^{\frac{k(k-1)}{2}} b^{\frac{k(k+1)}{2}} \qquad (5.11)$$

Theorem 5.3. *[1] The tail of the (2,2k+1) torus knot is given by* $T_K(A^4) = f(-A^{8k}, -A^4)$*, where* f *is the Ramanujan Theta function.*

In particular, note that the Tail of the trefoil (the (2,3)-torus knot) is

$$T_{3_1}(A^4) = f(-A^8, -A^4) = (A^4; A^4)_\infty \qquad (5.12)$$

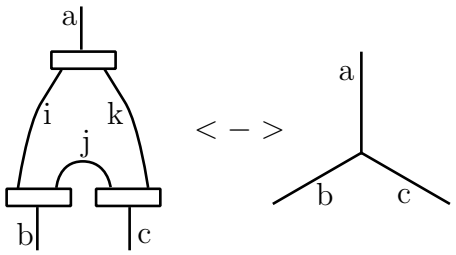

FIGURE 5.4: Transformation to Trivalent Graph Notation

Theorem 5.4. *[1] The tail of the (2,2k) torus link is given by* $T_L(A^4) = \Psi(A^{4(2k-1)}, A^4)$*, where* Ψ *is the False Theta function.*

In particular, note that the tail of the (2,4)-torus link is $\Psi(A^{12}, A^4)$.

5.3 Relations Involving the Tails of Multiple Torus Links

The following work was inspired by a question of Robert Osburn, who wished to understand how the tail of the $(2, 4)$-torus link was related to that of the $(2, 3)$-torus knot. Once can ask the more general question concerning how the tails of $(2, n)$- and $(2, m)$-torus links compare for arbitrary n and m.

In order to attack this problem, we will need to look at the bubble skein element studied in detail in [9]. In order to do so, we will employ the trivalent graph notation used in [15]. See Figure 5.4 for details on how to convert from one form to the other. In the remaining diagrams throughout this chapter, any unmarked strands or edges are assumed to be labelled n.

Lemma 5.5.

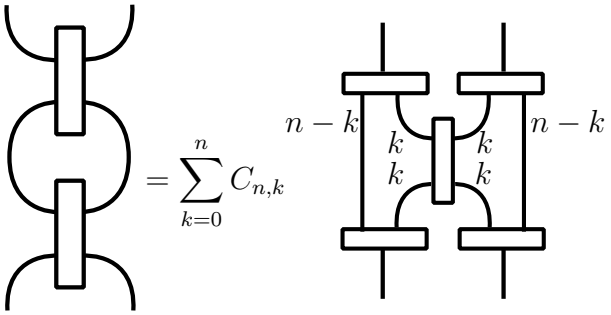

(5.13)

where $C_{n,k} = \frac{\Delta_{2k}\Theta(k,k,2n-k)}{\Theta(k,k,n-k)^2}$.

Proof. We first convert the bubble skein element into the trivalent graph notation of [15], as shown in Figure 5.4. It is easier to see this equality working backward; convert the trivalent graph into a skein element, and collapse the Jones-Wenzl Idempotents using Property 5.7. We then fuse the two edges labelled $2n$ according to the formula shown on p. 367 of [15]. We proceed to remove the triangles using another identity from the same page of [15], and finally recognize that the final graph is equivalent to the skein element in the statement of the lemma.

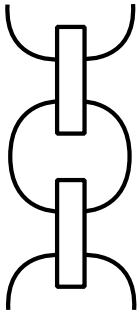

$=$

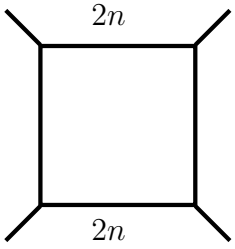

$$= \sum_{k=0}^{n} \frac{\Delta_{2k}}{\Theta(k,k,2n-k)}$$

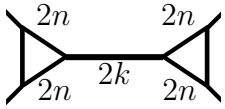

$$= \sum_{k=0}^{n} \frac{\Delta_{2k}\Theta(k,k,2n-k)}{\Theta(k,k,n-k)^2}$$

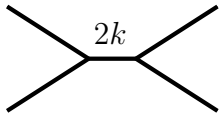

In the penultimate step, we use the fact that the tetrahedral coefficient that appears is a degenerate case, and reduces to a simple theta function. □

Using this lemma, we are able to show the following interesting identity relating the Ramanujan Theta function, the False Theta function, and a combinatorial sequence related to corner partitions of integers.

Theorem 5.6.

$$\Psi(A^{12}, A^4) = f(-A^8, -A^4)^2 + (A^4; A^4)_\infty^2 \sum_{k=0}^{\infty} d_k A^{4k} \tag{5.14}$$

where the coefficient d_k counts the number of planar partitions of k with only one row and column.

Proof. We will use the notation $\stackrel{n}{=}$ to denote that the two quantities are $4n$-equivalent. That is, after shifting each side independently by an appropriate power of A so that the result is a polynomial whose constant term is nonzero, the first $4n$ nonzero coefficients of the two sides agree. Recall that the tail of the $(4,2)$-torus link is equal to the left hand side of the equation. As such, we begin by looking at the skein element whose first n coefficients match that of this evaluation of the False Theta function.

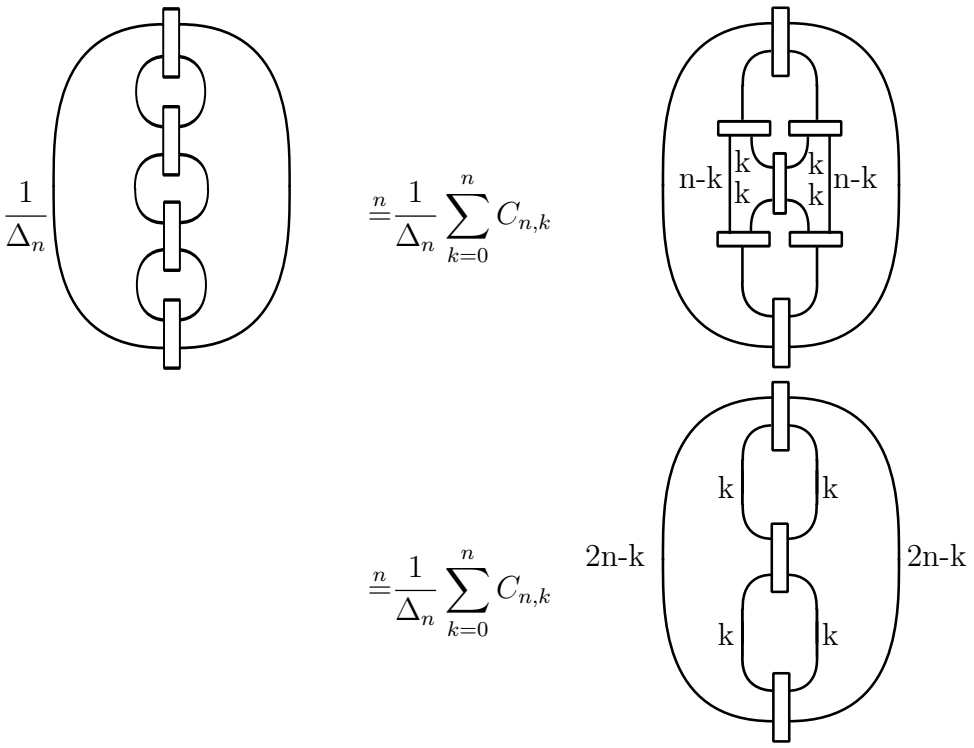

The diagram in the final term of the summation ($k = n$) is the skein element that represents the Tail of the (2,3)-torus knot, otherwise known as the trefoil. In all cases, the skein element actually evaluates to $\Theta(k, k, 2n-k)$. Proceeding with the calculation, we get that

$$\Psi(A^{12}, A^4) \stackrel{n}{=} \frac{C_{n,n}\Theta(n,n,n)}{\Delta_n} + \frac{1}{\Delta_n}\sum_{k=0}^{n-1} C_{n,k}\Theta(k,k,2n-k)$$

Substituting the formula for $C_{n,k}$ yields

$$\Psi(A^{12}, A^4) \stackrel{n}{=} \frac{\Delta_{2n}\Theta(n,n,n)^2}{\Delta_n\Theta(n,n,0)^2} + \sum_{k=0}^{n-1} \frac{\Delta_{2k}\Theta(k,k,2n-k)^2}{\Delta_n\Theta(k,k,n-k)^2}$$

We'll use the following identity several times throughout these calculations. These can be verified directly using the definitions, but it is more useful to consider each side of the equation as the value of a particular skein element and use the graphical properties of the Jones-Wenzl Idempotent to show the equality.

$$\Delta_{2k} = \Theta(k,k,0) = \Theta(2k,0,0) \tag{5.15}$$

We are thus able to write

$$\Psi(A^{12}, A^4) \stackrel{n}{=} \frac{\Theta(n,n,n)^2}{\Theta(n,0,0)\Theta(n,n,0)} + \sum_{k=0}^{n-1} \frac{\Delta_{2k}\Theta(k,k,2n-k)^2}{\Delta_n\Theta(k,k,n-k)^2}$$

Applying the definition of Θ, we write this as

$$\begin{aligned}\Psi(A^{12}, A^4) \stackrel{n}{=} &\frac{(-1)^n A^{-6n}(A^4;A^4)_n^7 (A^4;A^4)_{3n+1}^2}{(A^4;A^4)_{2n}^5 (A^4;A^4)_{n+1}(A^4;A^4)_{2n+1}} + \\ &\sum_{k=1}^{n-1} \frac{\Delta_{2k} A^{-4n}(A^4;A^4)_n^4 (A^4;A^4)_{2n-k}^2 (A^4;A^4)_{2n+k+1}^2}{\Delta_n (A^4;A^4)_{2n}^4 (A^4;A^4)_{n-k}^2 (A^4;A^4)_{n+k+1}^2}\end{aligned} \tag{5.16}$$

Consider the following quantity

$$\frac{(A^4;A^4)_n}{(A^4;A^4)_{2n}} = \frac{\prod_{j=0}^{n-1}(1-A^{4j})}{\prod_{j=0}^{2n-1}(1-A^{4j})} = \frac{1}{\prod_{j=1}^{n}(1-A^{4(n+j)})} = 1 + \mathcal{O}(A^{4(n+1)})$$

Similar calculations reveal that

- $\frac{(A^4;A^4)_{3n+1}}{(A^4;A^4)_{2n+1}} = 1 + \mathcal{O}(A^{4(2n+2)})$
- $\frac{(A^4;A^4)_{3n+1}}{(A^4;A^4)_{n+1}} = 1 + \mathcal{O}(A^{4(n+2)})$
- $\frac{(A^4;A^4)_{3n-k+1}}{(A^4;A^4)_{2n-k+1}} = 1 + \mathcal{O}(A^{4(2n-k+2)}) = 1 + \mathcal{O}(A^{4(n+2)})$

We can thus rewrite the first term in Equation 5.16 as

$$(-1)^n A^{-6n}(A^4;A^4)_n^2(1 + \mathcal{O}(A^{4(2n+2)})(1 + \mathcal{O}(A^{4(n+2)})(1 + \mathcal{O}(A^{4(n+1)}))^5 \tag{5.17}$$

$$= (-1)^n A^{-6n}(A^4;A^4)_n^2(1 + \mathcal{O}(A^{4(n+1)})) \tag{5.18}$$

We now turn our attention to the second part of the Equation 5.16. For ease of notation, define

$$F(n) = (A^4;A^4)_n^2 \sum_{k=0}^{n-1} \frac{\Delta_{2k} A^{-4n}(A^4;A^4)_n^2(A^4;A^4)_{2n-k}^2(A^4;A^4)_{2n+k+1}^2}{\Delta_n(A^4;A^4)_{2n}^4(A^4;A^4)_{n-k}^2(A^4;A^4)_{n+k+1}^2} \tag{5.19}$$

As before, note that

- $\frac{(A^4;A^4)_{2n+k+1}}{(A^4;A^4)_{n+k+1}} = 1 + \mathcal{O}(A^{4(n+k+2)}) = 1 + \mathcal{O}(A^{4(n+2)})$
- $\frac{(A^4;A^4)_{2n-k}}{(A^4;A^4)_{2n}} = 1 + \mathcal{O}(A^{4(2n-k+1)}) = 1 + \mathcal{O}(A^{4(n+1)})$

We can write

$$F(n) = (A^4;A^4)_n^2 \sum_{k=0}^{n-1} (1 + \mathcal{O}(A^{4(n+1)}))S(n,k) \tag{5.20}$$

where

$$S(n,k) = \frac{\Delta_{2k} A^{-4n}}{\Delta_n(A^4;A^4)_{n-k}^2} \tag{5.21}$$

Then,

$$F(n) = (A^4;A^4)_n^2 \sum_{k=0}^{n-1} S(n,k) - (A^4;A^4)_n^2 \sum_{k=0}^{n-1} \mathcal{O}(A^{4(n+2)}) S(n,k) \tag{5.22}$$

We will show that only the first sum contributes to the tail of F(n). To do so, we need to check that the minimal degree of any summand on the right is at least $4n$ greater than the minimal degree of the entire sum on the left. To do this, we now turn our attention to the quantity $S(n,k)$. We will need to use the fact that $\frac{1}{(A^4;A^4)_{n-k}^2} = 1 + \mathcal{O}(A^4)$.

$$\begin{aligned}
S(n,k) =& \frac{A^{-4n}\Delta_{2k}}{(A^4;A^4)_{n-k}^2 \Delta_n} && (5.23)\\
=& \frac{A^{-4n}\Theta(2k,0,0)}{(A^4;A^4)_{n-k}^2 \Theta(n,0,0)} && (5.24)\\
=& \frac{(-1)^n A^{2n-4k}(A^4;A^4)_{2k+1}(A^4;A^4)_n}{(A^4;A^4)_{n-k}^2 (A^4;A^4)_{2k}(A^4;A^4)_{n+1}} && (5.25)\\
=& \frac{(-1)^n A^{2n-4k}(1-A^{4(2k+1)})}{(A^4;A^4)_{n-k}^2 (1-A^{4(n+1)})} && (5.26)\\
=& (-1)^n A^{2n-4k}(1-A^{4(2k+1)})(1+\mathcal{O}(A^4)) \sum_{j=0}^{\infty} A^{4j(n+1)} && (5.27)
\end{aligned}$$

From this, we see that the minimal degree over all summands in the first sum in Equation 5.22 appears in only a single term, when k is maximized. There is no cancellation that may occur, so we have now shown that

$$F(n) = (A^4;A^4)_n^2 \sum_{k=0}^{n-1} \frac{\Delta_{2k} A^{-4n}}{\Delta_n (A^4;A^4)_{n-k}^2} + \text{Higher order terms} \tag{5.28}$$

Reindex this via the transformation $k \to (n-k)$ to get

$$F(n) = (A^4;A^4)_n^2 \sum_{k=1}^{n} \frac{\Delta_{2(n-k)} A^{-4n}}{\Delta_n (A^4;A^4)_k^2} + \text{Higher order terms} \tag{5.29}$$

Observe that

$$\frac{\Delta_{2(n-k)}}{\Delta_n} = \frac{(-1)^n A^{4k-2n}(1 - A^{4(2n-2k+1)})}{(1 - A^{4(n+1)})} \tag{5.30}$$

Substituting this into Equation 5.29 we get

$$\begin{aligned}
F(n) =& \frac{(-1)^n A^{-6n}(A^4; A^4)_n^2}{(1 - A^{4(n+1)})} \sum_{k=1}^{n} \frac{(A^{4k} - A^{4(2n-k+1)})}{(A^4; A^4)_k^2} + \text{Higher order terms} \\
=& (-1)^n A^{-6n}(A^4; A^4)_n^2 (1 - \mathcal{O}(A^{4(n+1)})) \sum_{k=1}^{n} \frac{(A^{4k} - A^{4(2n-k+1)})}{(A^4; A^4)_k^2} + \text{HOT} \\
=& (-1)^n A^{-6n}(A^4; A^4)_n^2 \sum_{k=1}^{n} \frac{(A^{4k} - \mathcal{O}(A^{4(n+1)}))}{(A^4; A^4)_k^2} + \text{HOT} \\
=& (-1)^n A^{-6n}(A^4; A^4)_n^2 \sum_{k=1}^{n} \frac{A^{4k}}{(A^4; A^4)_k^2} + \text{HOT}
\end{aligned}$$

We can now put this together with Equation 5.18 to get

$$\Psi(A^{12}, A^4) \stackrel{n}{=} (-1)^n A^{-6n}(A^4; A^4)_n^2 + (-1)^n A^{-6n}(A^4; A^4)_n^2 \sum_{k=1}^{n} \frac{A^{4k}}{(A^4; A^4)_k^2} \tag{5.31}$$

Shifting by $(-1)^n A^{-6n}$ and relabelling the first term in terms of the Theta function yields the result

$$\Psi(A^{12}, A^4) \stackrel{n}{=} f(-A^8, -A^4)^2 + (A^4; A^4)_n^2 \sum_{k=1}^{n} \frac{A^{4k}}{(A^4; A^4)_k^2} \tag{5.32}$$

Let us investigate the terms in the summation above. Writing it as a series, we can compare the sequence of coefficients with the Online Encyclopedia of Integer Sequences (OEIS) to discover that they appear to match sequence A006330. In fact, a generating function is given for this sequence, and it matches our summation exactly. The k^{th} coefficient of this series gives the number of corner partitions of k.

Definition 5.7. *A corner partition of k is a pair of ordered positive integer vectors $(a_1, a_2, \ldots a_r)$ and $(a_1, b_2, \ldots, b_s)$ such that*

1. $a_1 \geq a_2 \geq \ldots \geq a_r$

2. $a_1 \geq b_2 \geq \ldots \geq b_2$

3. $\Big(\sum_{n=1}^{r} a_n\Big) + \Big(\sum_{m=2}^{s} b_m\Big) = k$

So, we have established the identity relating the tails of the $(2,4)$-torus link, the $(2,3)$-torus knot, and the sequence counting corner partitions of positive integers.

□

We conclude this chapter with a general form of the previous computation, yielding a skein relation relating the tail of the $(2,m)$-torus knot (resp. link) with that of the $(2,m-2)$-torus knot (link).

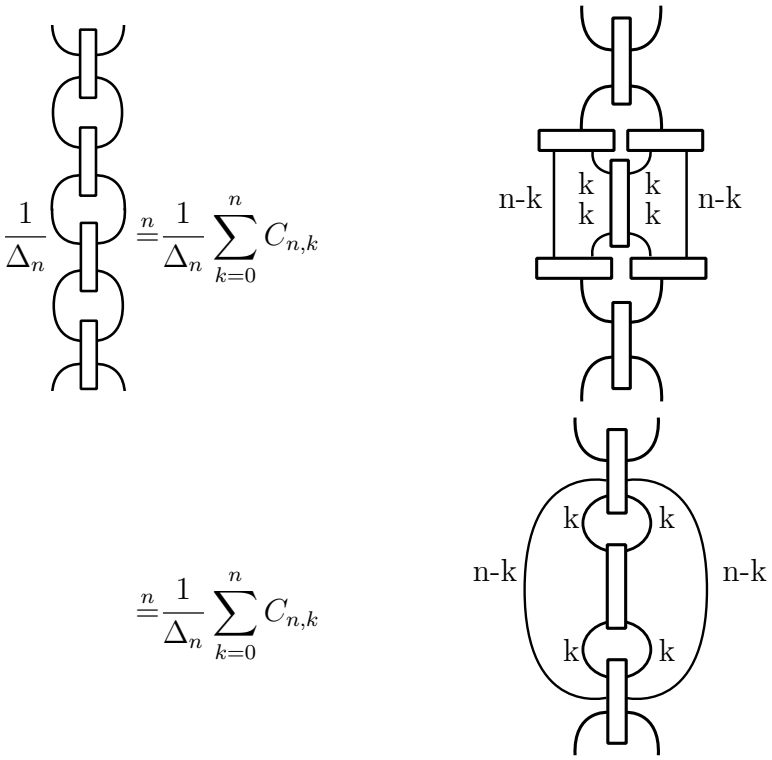

Here, observe that we have extra strands on either side labelled $n-k$. In the preceeding example, we were able to merge these with the strands connecting the top and bottom, but that is not possible in this more general setting. In order to

resolve this, we will rewrite the Jones-Wenzl Idempotent f^{2k} in the center of the diagram in terms of another basis, shown in Figure 5.5.

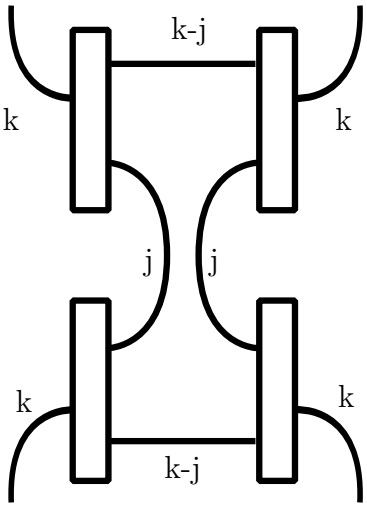

FIGURE 5.5: Partial Basis for TL_{2k}

This collection of diagrams does not form a full basis of TL_{2k}, but it is sufficient to express the term about which we are concerned. Rather than deriving the necessary coefficients, we can combine this calculation with the one above to write the bubble skein element from Lemma 5.5 in terms of this set. This is given in Theorem 4.11 of [10].

Theorem 5.8. *[10]*

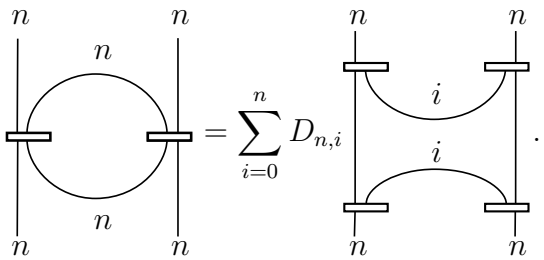

(5.33)

where

$$D_{n,i} = \frac{(-A^2)^{i(i-1)}(A^4;A^4)_n \prod_{j=0}^{n-i-1} \Delta_{n-j-1}\Delta_{3n-i-j} \prod_{s=0}^{i-1} \Delta_{n-s-1}^2}{(A^4;A^4)_i (A^4;A^4)_{n-i} \prod_{t=0}^{n-1} \Delta_{2n-t-1}^2}$$

Using this relation, we get

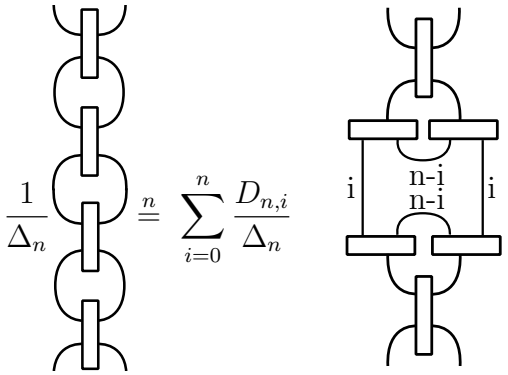

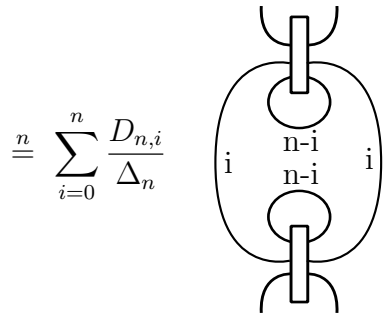

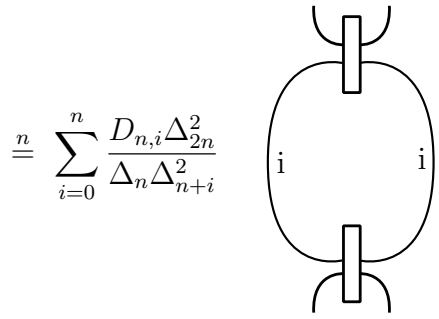

As before, we recognize that the last term of this sum corresponds to the tail of torus knot (resp. link) with two fewer crossings.

Chapter 6
Conclusion

The results of the previous chapter are very much dependent on the natural finite-order symmetries of the links involved. In particular, a $(2, m)$-torus link is both 2- and m-periodic, with the necessary diffeomorphism given by simply applying the appropriate rotation to the corresponding factor of the embedding torus $S^1 \times S^1$, sitting inside S^3 as a trivial genus-one Heegaard splitting surface. Without this repetitive structure, the skein-theoretic model would not be possible. Ongoing work includes an attempt to apply this to classes of knots that have this local structure, but do not necessarily support any global symmetry; pretzel knots are the next natural objects to investigate.

The chapter on periodic links gives a technique for detecting *asymmetry* of links, as the main theorem provides an obstruction to periodicity rather than a detector of the property. There are a great many avenues for further study using this work; in particular, current work is being undertaken to use this model to prove a conjecture that any odd prime period of an alternating link must divide the crossing number. There is hope of giving a stronger result, by extending this conjecture to include all adequate links.

Appendix A: Periodic Link Obstructions

Herein is included a brief set of Mathematica commands that can be used to calculate the obstruction to periodicity arising from the Kauffman Polynomial of links. The code contained in this appendix is compatible with Mathematica v. 10 and requires the package KnotTheory that can be downloaded from [2]. At the end of the appendix, a brief summary of the effectiveness of the obstruction for low-crossing prime knots and links is provided.

First, import the KnotTheory package.

```
<<KnotTheory`;
```

The following function takes as input a positive prime integer p, and two Laurent polynomials in variable q whose lower degrees are bounded by $(-200 * p)$. It outputs the difference of the two polynomials in the quotient ideal defined in the statement of Theorem 3.1.

```
CheckPer[funct1_, funct2_, p_] := Module[
    (*Declares local variables used in the scope of this function.*)
  {num, mirNum, modQuot, mirModQuot},
    (*Shifts the numerator of funct1, funct2 to create polynomials.*)
  num = Numerator[q^(200*p)*funct1];
  mirNum = Numerator[q^(200*p)*funct2];
    (*Evaluate these polynomials in the relevant quotient ideal.*)
```

modQuot = PolynomialMod[num[[1]], $q^{2*p} - 1$, Modulus ->p];

mirModQuot = PolynomialMod[mirNum[[1]], $q^{2*p} - 1$, Modulus ->p];

(*Output the difference of these quotients.*)

modQuot - mirModQuot

]

Next, provide the inputs for the desired series of calculations and initialize variables:

(*Specialization for the first variable.*)

a[q_] := $I * q$;

(*Specialization for the second variable.*)

z[q_] := $I * q - I * q^{-1}$;

(*Order of periodicity for which you wish to test.*)

testPrime = 11;

(*KnotList can by any list of knots that you wish to check.*)

KnotList := AllKnots[{1, 5}];

(*PolyList will store all knots that are positively obstructed.*)

PolyList = {};

(*Create an variable to index the while loop.*)

i = 1;

The following while loop will check every element of the KnotList for obstruction.

```
While[i <= Length[KnotList],
    (*Compute the Kauffman Polynomial for the specified knot.*)
  p11[a_, z_] := Kauffman[KnotList[[i]]][a, z];
    (*Specialize to the single-variable form of the obstruction.*)
  p12[q_] := Together[p11[(a[q])^-1, z[q]]];
    (*Give the specialized form for the mirror image.*)
  p13[q_] := Together[p11[a[q], z[q]]];
    (*Calculate the difference between the two in the quotient ideal.*)
  temp = CheckPer[p12[q], p13[q], testPrime];
    (*If temp is nonzero, condition evaluates to "neither true nor false".*)
  If[temp == 0,,,
    AppendTo[PolyList, KnotList[[i]]];
  ]
    (*Increment the index of the while loop.*)
  i++;
]
```

Finally, print the results. For large lists, it is recommended that you do not print the entire list, but instead only the length to get a count of the number of obstructions.

```
Length[PolyList]
```

3

PolyList

{*Knot[3, 1], Knot[5, 1], Knot[5, 2]*}

In order to evaluate links, some slight changes to the code are required. This results from the internal structure of the underlying dataset. As the underlying algorithm remains unchanged, the code is provided below without comments. The reader should note that data are imported from the linkinfo database saved as "linkinfo_data_complete.xlsx" in the home directory, which can be downloaded directly from [5]. The following block uses the same initializations as the program for knots, so those are not reproduced here.

```
<<KnotTheory`;
```

This function generates a list of links, drawn directly from the linkinfo database.

```
GenLinkList[max_, min_] := Module[
  {list},
  list :=    Import["linkinfo_data_complete.xlsx",
    {"Data", 1, Range[min + 2, max + 2], {1, 7}}
  ];
  list
]
```

We proceed to automate the computation of the obstruction for a set of parameters. Here, $n1$ and $n2$ are used to determine the range of links that we wish to evaluate, and p is the order of periodicity being investigated. The output as written will give a count of the number of obstructions encountered in the given set, but the last line of code can easily be modified to display the full list of links.

```
CheckLinks[n1_, n2_, p_] := Module[
  {linkList, polyList, poly, num, quot, polyMirror, numMirror, quotMirror, i},
  linkList := GenLinkList[n1, n2];
  polyList := {};
  i = 1;
  While[i <= Length[linkList],
    p11[a_, z_] := Kauffman[ToExpression[linkList[[i]][[2]]]][a, z];
    poly = Together[Expand[Together[p11[(a[q])^-1, z[q]]]]];
    num := Together[q^(200*p)*poly];
    quot = PolynomialMod[num[[1]], q^(2*p) - 1, Modulus ->p];
    polyMirror = Together[Expand[Together[p11[a[q], z[q]]]]];
    numMirror = Together[q^(200*p)*polyMirror];
    quotMirror = PolynomialMod[numMirror[[1]], q^(2*p) - 1, Modulus ->p];
    If[quot - quotMirror == 0, , ,
      AppendTo[polyList, linkList[[i]][[1]]];
    ];
    i++;
  ]
  Length[polyList]
]
```

We conclude this section with two tables summarizing the usefulness of the obstruction on knots and links of low crossing numbers.

Crossing Number	Total:	Obstructed: p=3:	Obstructed: p=5:	Obstructed: p=7:	Obstructed: p=11:
3	1	0	1	1	1
4	1	0	0	0	0
5	2	0	1	2	2
6	3	0	2	2	2
7	7	0	7	6	7
8	21	0	14	15	16
9	49	0	39	48	48
10	165	0	120	150	151
11	552	0	434	545	550
≤ 11	801	0	618	769	777

FIGURE 6.1: Summary of Obstruction for Knots

Crossing Number	Total Un/Oriented:	Obstructed: p=3:	Obstructed: p=5:	Obstructed: p=7:
2	1/2	0	2/2	1/2
4	1/2	0	1/2	1/2
5	1/2	0	2/2	1/2
6	6/18	0	4/13	5/13
7	9/20	0	9/19	9/20
8	29/96	0	18/45	28/83
≤ 8	47/140	0	36/83	45/122

FIGURE 6.2: Summary of Obstruction for Links

Appendix B:

Here we detail the computer-aided process used to discover the singular tangle operator extending the Kauffman Bracket. All code was written in Mathematica v.10. Throughout this section, we will use the notation $\phi = (A^4 - 1)$. We begin by defining the variables and inputs.

First, the singular R-matrix:

$$\text{R1} = \begin{pmatrix} x & b & c & d \\ e & f & g & h \\ k & l & m & n \\ o & p & q & s \end{pmatrix};$$

Quantum R-matrix and its inverse:

$$R = \begin{pmatrix} A & 0 & 0 & 0 \\ 0 & 0 & A\text{^}(-1) & 0 \\ 0 & A\text{^}(-1) & A - A\text{^}(-3) & 0 \\ 0 & 0 & 0 & A \end{pmatrix};$$

RInv = Inverse[R];

Identity Matrix (input appropriate dimension):

II = IdentityMatrix[2];

Define the cup and cap operators.

cup = $\{\{0\}, \{A\}, \{-A\text{^}(-1)\}, \{0\}\}$;

cap = $\left\{\left\{0, -A, \frac{1}{A}, 0\right\}\right\}$;

We will begin by determining the form of the singular R-matrix dictated by the RSIII-2 move.

First, compute the left hand side of Equation 4.5 and display the results.

S1 = Together[

KroneckerProduct[R, II].KroneckerProduct[II, R1].KroneckerProduct[RInv, II]

];

S1//MatrixForm

$$\begin{pmatrix} x & b & -\phi c & -\phi d & A^2 c & A^2 d & 0 & 0 \\ e & f & -\phi g & -\phi h & A^2 g & A^2 h & 0 & 0 \\ 0 & 0 & x & b & 0 & 0 & \frac{c}{A^2} & \frac{d}{A^2} \\ 0 & 0 & e & f & 0 & 0 & \frac{g}{A^2} & \frac{h}{A^2} \\ \frac{k}{A^2} & \frac{l}{A^2} & -\frac{\phi(m-x)}{A^2} & \frac{\phi(b-n)}{A^2} & m & n & \frac{\phi c}{A^4} & \frac{\phi d}{A^4} \\ \frac{o}{A^2} & \frac{p}{A^2} & \frac{\phi(e-q)}{A^2} & \frac{\phi(f-s)}{A^2} & q & s & \frac{\phi g}{A^4} & \frac{\phi h}{A^4} \\ 0 & 0 & A^2 k & A^2 l & 0 & 0 & m & n \\ 0 & 0 & A^2 o & A^2 p & 0 & 0 & q & s \end{pmatrix}$$

Do the same for the RHS of Equation 4.5.

S2 = Together[

KroneckerProduct[II, RInv].KroneckerProduct[R1, II].KroneckerProduct[II, R]

];

S2//MatrixForm

$$\begin{pmatrix} x & \frac{b}{A^2} & \frac{\phi b}{A^4} & 0 & c & \frac{d}{A^2} & \frac{\phi d}{A^4} & 0 \\ A^2 e & f & \frac{\phi(f-x)}{A^2} & -\phi b & A^2 g & h & -\frac{\phi(c-h)}{A^2} & -\phi d \\ 0 & 0 & x & A^2 b & 0 & 0 & c & A^2 d \\ 0 & 0 & \frac{e}{A^2} & f & 0 & 0 & \frac{g}{A^2} & h \\ k & \frac{l}{A^2} & \frac{\phi l}{A^4} & 0 & m & \frac{n}{A^2} & \frac{\phi n}{A^4} & 0 \\ A^2 o & p & -\frac{\phi(k-p)}{A^2} & -\phi l & A^2 q & s & -\frac{\phi(m-s)}{A^2} & -\phi n \\ 0 & 0 & k & A^2 l & 0 & 0 & m & A^2 n \\ 0 & 0 & \frac{o}{A^2} & p & 0 & 0 & \frac{q}{A^2} & s \end{pmatrix}$$

Combine the LHS and RHS to generate a list of expressions.

Equations = Flatten[S1 − S2, 2];

Set these expressions equal to zero to get a system of equations that the entries of the singular R-matrix must satisfy.

Equ = Table[Equations[[i]] == 0, {i, 1, Length[Equations]}];

Eliminate any redundancy in this set of equations. The output set is quite large, so the set of equations is partially suppressed in this document.

Finalset = DeleteCases[DeleteDuplicates[Equ], True];

Finalset//MatrixForm;

$$\left(\begin{array}{c} b-\frac{b}{A^2}==0 \\ -\frac{\phi b}{A^4}-\phi c==0 \\ -\phi d==0 \\ -c+A^2c==0 \\ -\frac{d}{A^2}+A^2d==0 \\ -\frac{\phi d}{A^4}==0 \\ e-A^2e==0 \\ -\phi g-\frac{\phi(f-x)}{A^2}==0 \\ \phi b-\phi h==0 \\ -h+A^2h==0 \\ \frac{\phi(c-h)}{A^2}==0 \\ \ldots \\ -\frac{\phi l}{A^4}-\frac{\phi(m-x)}{A^2}==0 \\ \frac{\phi(b-n)}{A^2}==0 \\ n-\frac{n}{A^2}==0 \\ \frac{\phi c}{A^4}-\frac{\phi n}{A^4}==0 \\ \frac{\phi d}{A^4}==0 \\ \frac{o}{A^2}-A^2o==0 \\ -p+\frac{p}{A^2}==0 \\ \frac{\phi(k-p)}{A^2}+\frac{\phi(e-q)}{A^2}==0 \\ \phi l+\frac{\phi(f-s)}{A^2}==0 \\ \ldots \\ -\frac{o}{A^2}+A^2o==0 \\ -p+A^2p==0 \\ q-\frac{q}{A^2}==0 \end{array}\right)$$

Proceed to solve the system of equations and display the result.

solutions = Solve[Finalset, $\{x, b, c, d, e, f, g, h, k, l, m, n, o, p, q, s\}$];

solutions}//MatrixForm

$$\left(\begin{pmatrix} b \to 0 \\ c \to 0 \\ d \to 0 \\ e \to 0 \\ g \to -\frac{f}{A^2} + \frac{x}{A^2} \\ h \to 0 \\ k \to 0 \\ l \to -\frac{f}{A^2} + \frac{x}{A^2} \\ m \to \frac{f}{A^4} - \frac{\left(1-A^4\right)x}{A^4} \\ n \to 0 \\ o \to 0 \\ p \to 0 \\ q \to 0 \\ s \to x \end{pmatrix}\right)$$

Display the resulting singular R-matrix.

RS1 = Simplify[Flatten[R1/.solutions, 1]];

RS1//MatrixForm

$$\begin{pmatrix} x & 0 & 0 & 0 \\ 0 & f & \frac{-f+x}{A^2} & 0 \\ 0 & \frac{-f+x}{A^2} & \frac{f+\phi x}{A^4} & 0 \\ 0 & 0 & 0 & x \end{pmatrix}$$

Proceed similarly for the RSIII-1 move.

Compute the LHS of Equation 4.6 and display the results.

S3 = Together[

KroneckerProduct[RInv, II].KroneckerProduct[II, R1].KroneckerProduct[R, II]

];

S3//MatrixForm

$$\begin{pmatrix} x & b & 0 & 0 & \frac{c}{A^2} & \frac{d}{A^2} & 0 & 0 \\ e & f & 0 & 0 & \frac{g}{A^2} & \frac{h}{A^2} & 0 & 0 \\ -\phi k & -\phi l & x & b & -\frac{\phi(m-x)}{A^2} & \frac{\phi(b-n)}{A^2} & A^2 c & A^2 d \\ -\phi o & -\phi p & e & f & \frac{\phi(e-q)}{A^2} & \frac{\phi(f-s)}{A^2} & A^2 g & A^2 h \\ A^2 k & A^2 l & 0 & 0 & m & n & 0 & 0 \\ A^2 o & A^2 p & 0 & 0 & q & s & 0 & 0 \\ 0 & 0 & \frac{k}{A^2} & \frac{l}{A^2} & \frac{\phi k}{A^4} & \frac{\phi l}{A^4} & m & n \\ 0 & 0 & \frac{o}{A^2} & \frac{p}{A^2} & \frac{\phi o}{A^4} & \frac{\phi p}{A^4} & q & s \end{pmatrix}$$

Compute the RHS of Equation 4.6 and display the results.

S4 = Together[

KroneckerProduct[II, R].KroneckerProduct[R1, II].KroneckerProduct[II, RInv]

];

S4//MatrixForm

$$\begin{pmatrix} x & A^2 b & 0 & 0 & c & A^2 d & 0 & 0 \\ \frac{e}{A^2} & f & 0 & 0 & \frac{g}{A^2} & h & 0 & 0 \\ \frac{\phi e}{A^4} & \frac{\phi(f-x)}{A^2} & x & \frac{b}{A^2} & \frac{\phi g}{A^4} & -\frac{\phi(c-h)}{A^2} & c & \frac{d}{A^2} \\ 0 & -\phi e & A^2 e & f & 0 & -\phi g & A^2 g & h \\ k & A^2 l & 0 & 0 & m & A^2 n & 0 & 0 \\ \frac{o}{A^2} & p & 0 & 0 & \frac{q}{A^2} & s & 0 & 0 \\ \frac{\phi o}{A^4} & -\frac{\phi(k-p)}{A^2} & k & \frac{l}{A^2} & \frac{\phi q}{A^4} & -\frac{\phi(m-s)}{A^2} & m & \frac{n}{A^2} \\ 0 & -\phi o & A^2 o & p & 0 & -\phi q & A^2 q & s \end{pmatrix}$$

Generate a list of equations dictated by Equation 4.6. Again, some of the output has suppressed in this document.

SecondEquations = Flatten[S3 − S4, 2];

SecondEqu = Table[SecondEquations[[i]] == 0, {i, 1, Length[SecondEquations]}];

SecondFinalSet//MatrixForm

$$
\left(\begin{array}{c}
b - A^2 b == 0 \\
-c + \frac{c}{A^2} == 0 \\
\frac{d}{A^2} - A^2 d == 0 \\
e - \frac{e}{A^2} == 0 \\
-h + \frac{h}{A^2} == 0 \\
-\frac{\phi e}{A^4} - \phi k == 0 \\
-\phi l - \frac{\phi(f-x)}{A^2} == 0 \\
b - \frac{b}{A^2} == 0 \\
-\frac{\phi g}{A^4} - \frac{\phi(m-x)}{A^2} == 0 \\
\frac{\phi(c-h)}{A^2} + \frac{\phi(b-n)}{A^2} == 0 \\
-c + A^2 c == 0 \\
-\frac{d}{A^2} + A^2 d == 0 \\
-\phi o == 0 \\
\phi e - \phi p == 0 \\
e - A^2 e == 0 \\
\phi g + \frac{\phi(f-s)}{A^2} == 0 \\
\ldots \\
q - \frac{q}{A^2} == 0 \\
-\frac{\phi o}{A^4} == 0 \\
\frac{\phi(k-p)}{A^2} == 0 \\
-k + \frac{k}{A^2} == 0 \\
\frac{\phi k}{A^4} - \frac{\phi q}{A^4} == 0 \\
\frac{\phi l}{A^4} + \frac{\phi(m-s)}{A^2} == 0 \\
\ldots \\
\frac{\phi o}{A^4} == 0 \\
\frac{\phi p}{A^4} + \phi q == 0 \\
q - A^2 q == 0
\end{array}\right)
$$

Proceed to solve the system of equations.

SecondSolutions = Solve[SecondFinalSet, $\{x, b, c, d, e, f, g, h, k, l, m, n, o, p, q, s\}$];

Display the form of the singular R-matrix according to these solutions. Observe that the result in this case is identical to that dictated by the SRIII-2 move.

RS2 = Simplify[Flatten[R1/.SecondSolutions, 1]];

RS2//MatrixForm

$$\begin{pmatrix} x & 0 & 0 & 0 \\ 0 & f & \frac{-f+x}{A^2} & 0 \\ 0 & \frac{-f+x}{A^2} & \frac{f+\phi x}{A^4} & 0 \\ 0 & 0 & 0 & x \end{pmatrix}$$

Proceed to check if this singular R-matrix satisfies the RSI move, expressed algebraically in Equation 4.4.

Together@(RInv.RS1.R − RS1)=={{0, 0, 0, 0}, {0, 0, 0, 0}, {0, 0, 0, 0}, {0, 0, 0, 0}}

True

Confirm the product of the cup and cap.

cap.cup//MatrixForm

cup.cap//MatrixForm

$$\begin{pmatrix} -\frac{1}{A^2} - A^2 \end{pmatrix}$$

$$\begin{pmatrix} 0 & 0 & 0 & 0 \\ 0 & -A^2 & 1 & 0 \\ 0 & 1 & -\frac{1}{A^2} & 0 \\ 0 & 0 & 0 & 0 \end{pmatrix}$$

Check that the singular R-matrix decomposes into the form in Equation 4.15.

Together@{RS2} == Together@

$\left\{x * \text{KroneckerProduct}[\text{IdentityMatrix}[2], \text{IdentityMatrix}[2]] + \left(\frac{-f+x}{A^2}\right) * \text{cup.cap}\right\}$

True

Displayed in expanded form, this reads

$$\begin{pmatrix} x & 0 & 0 & 0 \\ 0 & f & \frac{-f+x}{A^2} & 0 \\ 0 & \frac{-f+x}{A^2} & \frac{f+\phi x}{A^4} & 0 \\ 0 & 0 & 0 & x \end{pmatrix} = x \begin{pmatrix} 1 & 0 & 0 & 0 \\ 0 & 1 & 0 & 0 \\ 0 & 0 & 1 & 0 \\ 0 & 0 & 0 & 1 \end{pmatrix} + \left(\frac{-f+x}{A^2}\right) * \begin{pmatrix} 0 & 0 & 0 & 0 \\ 0 & -A^2 & 1 & 0 \\ 0 & 1 & -\frac{1}{A^2} & 0 \\ 0 & 0 & 0 & 0 \end{pmatrix}$$

Check the conditions that are necessary to satisfy the Singular Cap Switch, expressed algebraically in Equation 4.7, and display the results.

Specialization = Solve[(KroneckerProduct[cap, II].KroneckerProduct[II, RS1] −

KroneckerProduct[II, cap].KroneckerProduct[RS1, II])==

$\{\{0,0,0,0,0,0,0,0,0\},\{0,0,0,0,0,0,0,0,0\}\}$]

$\{\{f \to x(1-A^2)\}\}$

Apply the solution to the singular R-matrix to complete the computation.

Flatten[RS1/.Specialization, 1]//MatrixForm

$$\begin{pmatrix} x & 0 & 0 & 0 \\ 0 & x - A^2 x & x & 0 \\ 0 & x & \frac{x - A^2 x + \phi x}{A^4} & 0 \\ 0 & 0 & 0 & x \end{pmatrix}$$

References

[1] C. Armond and O. T. Dasbach, *Rogers-ramanujan type identities and the head and tail of the colored jones polynomial*, 2011.

[2] D. Bar-Natan, S. Morrison, and et al., *The Knot Atlas*.

[3] G. Burde, H. Zieschang, and M. Heusener, *Knots*, vol. 5 of De Gruyter Studies in Mathematics, De Gruyter, Berlin, extended ed., 2014.

[4] C. Caprau and J. Tipton, *The kauffman polynomial and trivalent graphs*, (2011).

[5] J. C. Cha and C. Livingston, *Linkinfo: Table of knot invariants*, March 2017.

[6] O. T. Dasbach and C. Armond, *The head and tail of the colored jones polynomial for adequate knots*, 2013.

[7] T. Fiedler, *The jones and alexander polynomials for singular links*, 2007.

[8] P. J. Freyd and D. N. Yetter, *Braided compact closed categories with applications to low dimensional topology*, Advances in Mathematics, 77 (1989), pp. 156 – 182.

[9] M. Hajij, *The bubble skein element and applications*, Journal of Knot Theory and Its Ramifications, 23 (2014), p. 1450076.

[10] M. Hajij, *Knots, Skein Theory and Q-Series*, PhD thesis, Louisiana State University and Agricultural and Mechanical College, 2015.

[11] A. Hatcher, *Algebraic topology*, Cambridge University Press, Cambridge, 2002.

[12] S. Jabuka and S. Naik, *Periodic knots and heegaard floer correction terms*, 2013.

[13] L. H. Kauffman, *An invariant of regular isotopy*, Trans. Amer. Math. Soc., 318 (1990), pp. 417–471.

[14] W. B. R. Lickorish, *An introduction to knot theory*, vol. 175 of Graduate Texts in Mathematics, Springer-Verlag, New York, 1997.

[15] G. Masbaum and P. Vogel, 3*-valent graphs and the Kauffman bracket*, Pacific J. Math., 164 (1994), pp. 361–381.

[16] K. Murasugi, *On periodic knots*, Comment. Math. Helv., 46 (1971), pp. 162–174.

[17] K. Murasugi, *On symmetry of knots*, Tsukuba Journal of Mathematics, 4 (1980), pp. 331–347.

[18] K. Murasugi, *Jones polynomials of periodic links*, Pacific J. Math., 131 (1988), pp. 319–329.

[19] T. Ohtsuki, *Quantum invariants*, vol. 29 of Series on Knots and Everything, World Scientific Publishing Co., Inc., River Edge, NJ, 2002. A study of knots, 3-manifolds, and their sets.

[20] J. H. Przytycki, *On Murasugi's and Traczyk's criteria for periodic links*, Math. Ann., 283 (1989), pp. 465–478.

[21] J. H. Przytycki, *Fundamentals of kauffman bracket skein modules*, 1998.

[22] P. Traczyk, 10_{101} *has no period* 7*: a criterion for periodic links*, Proc. Amer. Math. Soc., 108 (1990), pp. 845–846.

[23] ——, *Periodic knots and the skein polynomial*, Invent. Math., 106 (1991), pp. 73–84.

[24] V. G. Turaev, *The Yang-Baxter equation and invariants of links*, Invent. Math., 92 (1988), pp. 527–553.

[25] ——, *Conway and kauffman modules of a solid torus*, Journal of Soviet Mathematics, 52 (1990), pp. 2799–2805.

[26] ——, *Operator invariants of tangles, and r-matrices*, Math. USSR-Izv., 35 (1990), pp. 411–444.

[27] Y. Yokota, *The Jones polynomial of periodic knots*, Proc. Amer. Math. Soc., 113 (1991), pp. 889–894.

[28] ——, *The Kauffman polynomial of periodic knots*, Topology, 32 (1993), pp. 309–324.

Vita

Kyle Istvan was born in Columbia, South Carolina. He finished his undergraduate studies at the University of Georgia in 2010. He earned a master of science degree in mathematics from Louisiana State University in 2011, and continued to pursue graduate studies in mathematics. He is currently a candidate for the degree of Doctor of Philosophy in mathematics at LSU.